الجمهورية الجـزائـريـة الديمـقراطـيـة الشـعـبيـــة
وزارة التعليم العـــالي والبـحـث العلمـي
PEOPLE 'S DEMOCRATIC REPUBLIC OF ALGERIA
MINISTERY OF HIGH EDUCATION AND SCIENTIFIC RESEARCH
جـامعة سـعد دحلـب البلـيـــدة1
UNIVERSITY OF SAAD DAHLEB BLIDA 1

كلية العلوم – دائرة الفيزياء
Faculty of science
Department of Physics

MASTER DIPLOMA THESIS
In physics

Option: Nanophysics

THEME

THERMAL ANNEALING EFFECT ON THERMAL EVAPORATED VANADIUM OXIDES THIN FILM

By:

BENHENNI Imen - BERROUANE Wassila

Jury Member:

Dr. A. HASSEIN-BEY	MCB,	U. Blida 1	President
Dr. H. TAHI	DR,	CDTA Baba Hassen	Examiner
Dr. S. LAFANE	MRB,	CDTA Baba Hassen	Advisor
A.L.S HASSEIN-BEY		U. Blida 1/CDTA Baba Hassen	Co-Advisor

2018 / 2019

Abstract

Vanadium oxide thin films have attracted considerable attention as potential candidates for many advanced applications such as: electrochromic devices; thermo chromic coatings; metal semiconductor transition materials; and electrodes for batteries. This diverse range of applications is made possible due to the several stable oxidation states of vanadium oxide (V_2O_5, VO_2, VO, and V_2O_3) which depend on the fabrication process, annealing treatment, and source material.

In this Study, vanadium oxide thin films are prepared by thermal evaporation method is deposited on glass substrate. The films are annealed under different temperatures from 400°C to 550°C for various times to obtain desired oxygen phases of vanadium oxide thin films. After appropriate annealing step, V_2O_5 structured thin films are reduced to mixture of lower oxygen states of vanadium oxide thin films which contains V_2O_5, VO_2 and VO_X .

Résumé

Les films minces d'oxyde de vanadium ont attiré une attention considérable en tant que candidats potentiels pour de nombreuses applications avancées telles que ; les dispositifs électrochromiques, les revêtements thermochromiques, les matériaux de transition métal semi-conducteur et les électrodes pour batteries. Cette diversité d'applications est rendue possible grâce aux différents états d'oxydation stables de l'oxyde de vanadium (V_2O_5, VO_2, VO, V_2O_3) qui dépendent du procédé de fabrication, du traitement de recuit et du matériau source.

Dans cette étude, les couches minces d'oxyde de vanadium sont préparées par évaporation thermique et déposées sur un substrat de verre. Les films sont recuits à différentes températures de 400°C à 550°C pendant plusieurs temps pour obtenir les phases d'oxygène souhaitées des films minces d'oxyde de vanadium. Après l'étape de recuit appropriée, les couches minces structurées de V_2O_5 sont réduites à un mélange de couches minces d'oxyde de vanadium à l'état d'oxygène inférieur qui contient V_2O_5, VO_2 et VO_X.

ملخص

جذبت طبقات رقيقة من أكسيد الفناديوم اهتمامًا كبيرًا كمرشحين محتملين للعديد من التطبيقات المتقدمة مثل: الأجهزة الكهرو ميكانيكية؛ الطلاء بالكروم الحراري .المواد الانتقال أشباه الموصلات المعدنية .وأقطاب للبطاريات .هذه المجموعة المتنوعة من التطبيقات أصبحت ممكنة بسبب العديد من حالات التأكسد المستقرة لأكسيد الفناديوم(V_2O_5 ، VO،VO_2 ، V_2O_3)والتي تعتمد على عملية التصنيع، معالجة الصلب، والمواد المصدر.

في هذه الدراسة، يتم تحضير أغشية رقيقة من أكسيد الفناديوم بطريقة التبخير الحراري التي يتم ترسيبها على الركيزة الزجاجية .يتم تقسية الأفلام تحت درجات حرارة مختلفة من 400 درجة مئوية إلى 550 درجة مئوية لعدة مرات للحصول على مراحل الأكسجين المرغوبة من أغشية رقيقة من أكسيد الفناديوم .بعد خطوة التلدين المناسبة، يتم تقليل الأفلام الرقيقة المهيكلة V_2O_5 إلى مزيج من حالات الأكسجين المنخفضة للأغشية الرقيقة بأكسيد الفناديوم والتي تحتوي علىV_2O_5 وVO_2وVO_X.

Acknowledgments

First, we would like to thank the two persons that Allah has blessed me with in our life; **Our Parents** who sacrificed their youth and energy, and gave us all their love and support to transform the lives they gave us into wonderful adventures. We are so glad and blessed to be able to wake up every day and see their smiles. We wish that we make them proud, and that they can finally pick up the fruits of their efforts.

Secondly, we would be more than glad to thank our advisor "**Dr. Slimane LAFANE**" and Co-advisor "**Asmaa Leila Sabeha HASEEIN-Bey**" for all the patience, time and efforts that they were so generous to give to us during the period of accomplishing this work and this allowed us to gain valuable knowledge, experience, confidence and a strong will to accomplish this work. We wish them all the success in all the projects that they are working on. Great thank to them for bringing valuable help by providing us with innovative solutions and encouraging us when facing problems.

We acknowledge warmly ionized medium & laser division especially the Laser matter interaction group also Microelectronics & Nanotechnology Division of the CDTA for the easiness and the good progress of work. The authors would like to thank **AMMI Ismail Dr. H. TAHI**. A great thank for **Dr. Fouaz LEKOUI** for his precious help and advices. We also thank FUNDAPL Laboratory / University of Blida 1 for SEM characterization notably Prof. **M.E.A BENAMAR**. We whole heartedly thank technicians of the CDTA and all that involve in this work by advice and helpful.

Above that, we would like to thank "**Dr. Abdelkader Hassein-Bey**" for the efforts that he put into opening the branch of Nano-physics, which allowed us to access this amazing field of "Microsystems". In addition to this, we thank him for the efforts that he put into teaching us for longer hours every day, several days a week, all of this to deliver us valuable information that we certainly found helpful in the work reported in this thesis. We would address our acknowledgements to the members of the jury, starting with the president of the jury "**Dr. A.Hassein-bey**", the examiner "**Dr. H.Tahi**", and the advisors "**Dr. S. Lafane**" and " **A.L. S Hassein-Bey**", for giving us the honor to examine this work, and for the time and efforts that they have taken to read and correct this manuscript. We will certainly not forget all the teachers that taught us through all these academic years.

At last not least, it is more than a pleasure to address our acknowledgement to our family members, friends and every person that gave us material and emotional support, just to push us to study and reach this level.

List of contents

CHAPTER III : EXPERIMENTAL PROCEDURE

CHAPTER IV : RESULTS AND DISCUSSIONS

List of figures

Chapter I

Chapter II

List of tables

General introduction

A semiconductor thin layer represents a new class of materials. The Interest that brings in the scientific community since the early 1980s is more and more growing. To meet a growing set of needs, a major research effort has been undertaken in recent years in several technological fields ranging from microelectronics, to transducer gas sensor optoelectronics. Thin layered vanadium oxide has generated considerable interest because of these characteristics (transparency, wide conductivity, stability Chemical, and ease of elaboration ...) which makes this material a serious candidate for different applications.

The development of science and technology has impoved many ways of thin film deposition technique over the time (PLD, electron beam deposition, sputtering…..) among that, one of the most basic and primitive process includes evaporation. Let's say, a mechanism for the deposition of very thin film of a material over a substrate is needed.

A syestematic study of the influence of thermal treatments of these thermally evaporated layers on their optical properties, structural, morphological and electrical remains a must for the understanding of physical phenomena and for the optimization of their performance for use in these devices.

The objective of our study is the preparation of thin layers of vanadium oxide by thermal evaporation from a powder of V_2O_5 followed by annealing under air at different temperatures. We try to optimize the annealing temperature in order to obtain good quality vanadium oxide films, And to study the effect of the annealing process on the films properties.

In this study, vanadium oxide thin films are prepared by thermal evaporation method and is deposited on amorphous glace. The films are annealed under different temperature from 400°C_550°C for various time to obtain desired oxygen phases of vanadium oxide thin films. After appropriate annealing step, V_2O_5 structured thin films are reduced to mixture of lower oxygen states of vanadium oxide thin films which contains V_2O_5, V_6O_{13}, and VO_2. Finally, the performance parameters such as sheet

resistance, TCR, and noise are measured to verify the quality of the developed vanadium oxide active layers.

Our memory will be articulated around chapters.

We dedicate the first chapter of this paper to some notions about vanadium oxide thin layers and then the presentation of some methods of elaborating these layers

In the second chapter, we make a general presentation of thin layers properties.

The experimental details and the technique of deposition of thin layers of vanadium oxide as well as characterization techniques is the subject of the third chapter.

In the fourth chapter, were group and discuss the Experiments results on the influence of thermal treatments on the composition, structure, morphology and electrical properties thin layers of vanadium oxide.

Chapter I

BACKGROUND

I.1 Introduction

Vanadium has an interesting property of existing in more than one stable oxidation state (multi-valency) and it forms as many as 15 oxide compounds such us VO_2, V_2O_3, V_2O_5, V_6O_{13} etc.… [1-2]. the vanadium oxides have several useful properties such as electro-chromic and thermo-chromic behaviour, metal to insulator transition and high temperature coefficient of resistance. Due to these technologically useful properties vanadium oxides have wide range of applications for example smart windows, vanadium oxide VO_2 is one of the most promising potential candidate for smart window materials due to its ability to reversibly transit from monoclinic VO_2 (M) to rutile VO_2(R) at near room temperature also vanadium oxide can be used as gas sensors and for electro chromic devices [3].

I.2 Vanadium

Vanadium was discovered in 1801 in Mexico City by A.M. Del Rio disputed, then rediscovered in 1831 by N. G. Selfström in Falun, Sweden [4]. Etymology of the name: comes from Vanadis, goddess of beauty in Scandinavian mythology.

Vanadium, ranked among the 22nd most widespread elements in all lithosphere, is located at low concentrations: 0.07% on average, up to 2%. Vanadium is found in nature as compoundschemicals found in more than 65 species of ores, is also found in rocks, in iron ores and in oil deposits. Vanadium is the chemical element of symbol V, atomic number 23 and electronic configuration [Ar] $3d^3$ $4s^2$ located in the 5th column of Mendeleev's table. In the crystal the vanadium atoms occupy the nodes of a cubic lattice at centered faces, in its crystalline structure the vanadium oxide is a semiconductor [4].

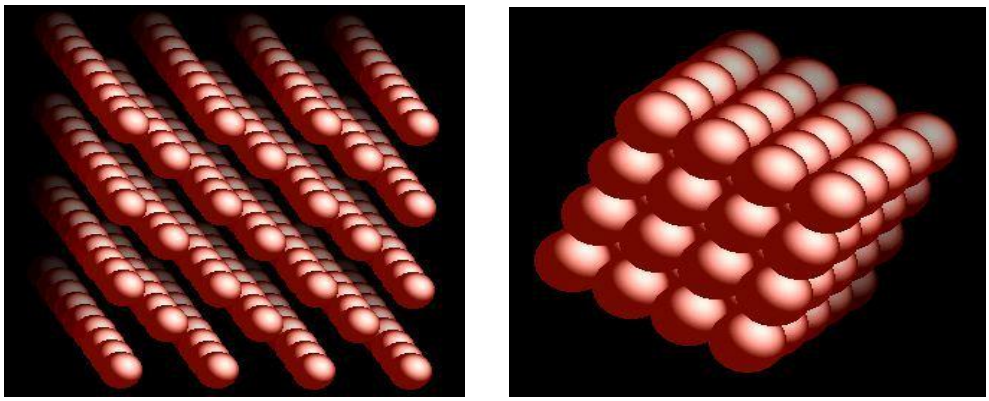

Fig.I-1: Crystalline structure of vanadium [5].

I.2.1 Vanadium extraction

The ore used is the patronite which consists of vanadium sulphide containing ironand nickel. The extraction of vanadium is ensured by the following operations: [4]

1. Ore beneficiation by physical method
2. Sulphide wire
3. Oxidative alkaline fusion in a reverberatory furnace: vanadium goes into the state of vanadate, the iron in the state of alkaline ferrite, the oxide NiO remains unaltered, and the vanadate is separates by density of iron and nickel.
4. After grinding, the slag containing vanadium is washed rationally: it provides a solution of $NaVO_3$ that is separated from insolubles (iron, nickel, ...)
5. The Meta vanadate solution is treated with ammonia, which precipitates NH_4VO_3little Soluble: other metals that have followed vanadium remain in solution
6. After several rushes to the state of NH_4VO_3 if necessary, vanadate is calcined:

$$2\ NH_4VO_3 \rightarrow V_2O_5 + 2\ NH_3 + H_2O$$

7. Aluminothermy treated V_2O_5 oxide provides 98% crude vanadium.

I.2.2 Physical properties

Pure vanadium is a greyish silver metal (solid at 298°K), soft and malleable. He possesses when it is pure of excellent mechanical characteristic and can work itself cold and hot, but small amounts of impurities, hydrogen, nitrogen and oxygen the make it

hard and brittle [4].Vanadium is available in many forms including foil, granules, powders and stems.

I.2.3 Chemical properties

- **Reaction of vanadium with air**

At room temperature, the vanadium metal hardly oxidizes in the air. By against, it reacts with the excessive oxygen O_2, during heating at 660 ° C. [4]

$4V\ (s) + 5O_2\ (g) \rightarrow 2V_2O_5\ (s)$ [yellow-orange]

- **Reaction of vanadium withhalogens**

Vanadium reacts with fluorine, F_2 during heating

$2V\ (s) + 5F_2\ (g) \rightarrow 2VF_5$ [colorless]

By raising the temperature, it reacts with the chlorine, forming VCl_4.

- **Reaction of vanadium with acids and bases**

It is resistant to non-oxidizing acids, but is strongly attacked by nitric acid or the water regales. It easily fixes hydrogen.

I.3 Vanadium oxides

In the environment, vanadium offers a complex chemistry. As a consequence of its multivalent character, it has a number of possible oxidation states (V^{+2}, V^{+3}, V^{+4}, V^{+5}), which form an extensive list of binary V−O systems. Some of them are grouped in the so-called “Magneli phases,” with stoichiometric formula V_nO_{2n-1}, and others in the Wadsley phases, with stoichiometric formula V_nO_{2n+1}.

The most commonly used phases, found in various applications due to their particular properties, are the VO, VO_2, V_2O_3, and V_2O_5 oxide phases. The figure bellow represent phase diagram vanadium-oxygen [10].

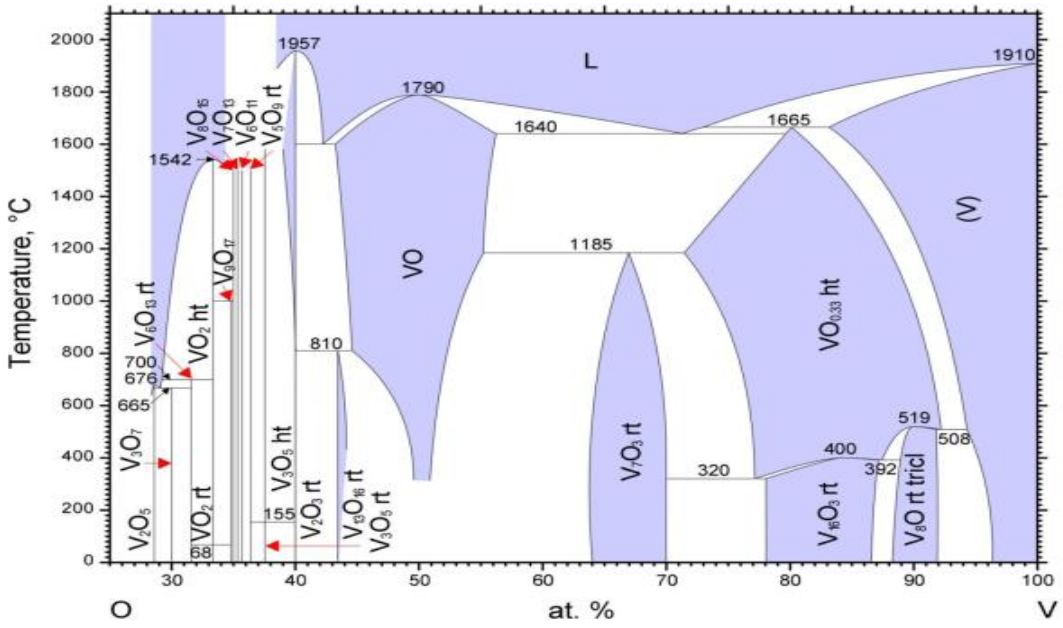

Fig.I-2: Phase Diagram vanadium-oxygen [20].

I.3.1 vanadium monoxide

VO is one of the many vanadium oxide phases with crystalline cubic structure and good electrical conductivity due to the partially filled conduction band and the delocalization of electrons in the 2 g orbital [7].

I.3.2 vanadium trioxide

V_2O_3 phase, like VO_2 compound, presents an abrupt conductivity change at a temperature around 160°K, evidenced of a metal-insulator transition. In addition, it presents a thermochromic behaviour in the infrared band [7].

I.3.3 vanadium pentoxide

V_2O_5 is the most stable of all vanadium oxide phases, and the preferred one to be used as thermoresistive material in microbolometer arrays for thermal imaging due to its high TCR value. Vanadium pentoxide is a semiconductor with a bandgap of 2.1–2.4 eV, which presents the following polymorphs: α-V_2O_5 (orthorhombic),

β-V_2O_5 (monoclinic or tetragonal), and γ-V_2O_5 (orthorhombic), being the α-polymorph the most stable one [9].

I.3.4 vanadium dioxide

VO_2 is an amphoteric compound with the unique property of changing from a semiconductor monoclinic phase to a (semi)metal tetragonal rutile phase at a temperature around 340°K and, therefore, its electrical resistivity together with the optical properties also change up to several orders of magnitude between these two states [8].

a. General characteristics of VO_2

Among the materials with insulating-to-metal phase transition, vanadium dioxide is one of the most studied in the literature. It was discovered more than 50 years ago by F. J. Morin [10]. This one highlighted its transition to a temperature close to the ambient temperature. VO_2 has very different physical properties on either side of the phase transition, which makes it possible to consider its integration into different devices for both electronic and optical applications.

b. Crystallographic structure

A different structural arrangement is observed on either side of the isolation-metal transition in VO_2. Indeed, vanadium dioxide passes from a monoclinic structure (M1) at low temperature to a quadratic structure / Rutile (R) at high temperature. **Figure.I-3** illustrates the VO_2 structures in both insulating and metallic states [12].

The monoclinic insulating phase **(Figure.I-3(a))** belonging to space group P21/c, is characterized by vanadium atoms forming pairs along the c-axis of the mesh. It is also characterized by the alternation of short (2,613 Å) and long (3,176 Å) distances from the V-V link, each pair formed by these links is "tilted" to form a zig-zag along the c axis of the mesh [13]. The mesh parameters a, b and c of the insulating phase of VO_2 are 5.7529 Å, 4.5263 Å and 5.3825 Å respectively.

The rutile structure is based on a simple quadratic mesh with the space group P42/mnm. Vanadium cations form a centred quadratic network, oxygen atoms form a deformed octahedron around a vanadium atom, such that four vanadium-oxygen distances are equivalent in one plane and two other distances are equivalent in the plane perpendicular thereto. The octahedrons share the same edge along the c-axis forming infinite chains. These chains have in common their vertices [13] (**Figure I-3(b)**).

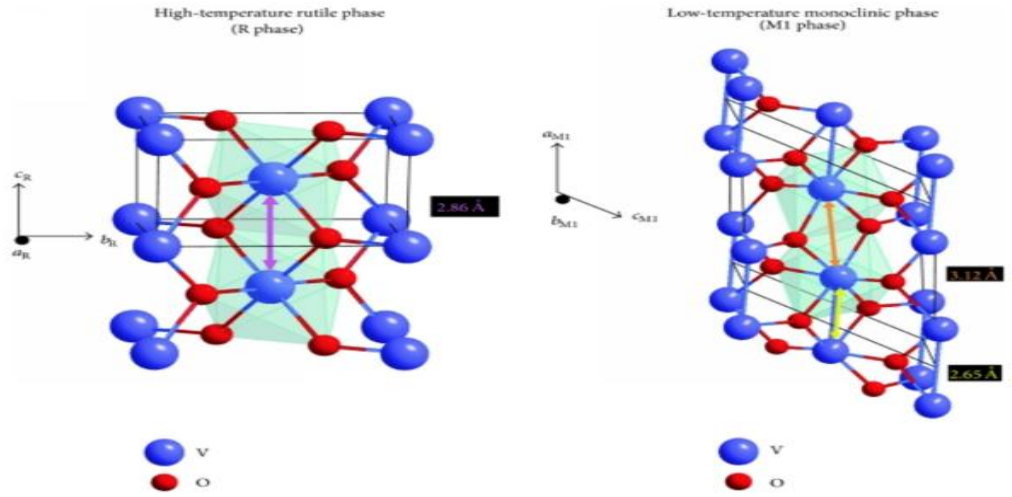

Fig.I-3: Low temperature monoclinic VO_2 (M1) structure and high temperature rutile (R) structure [6].

c. Band structure

During its transition from insulation to metal phase, the VO_2 band structure also changes. In the metallic state, the VO_2 structure consists of two bands; a 3d// binding band and an anti-binding band 3dπ*. By moving from the metal phase to the insulating phase during the TIM, the 3d// band is divided in two. We therefore find a filled binder strip with a lower energy called 3d// and another empty anti-binder strip with a higher energy called 3d//*. Finally, the binding strip 3dπ* is pushed to a higher energy. As a

result, a band gap and therefore a gap Eg of [0.6-0.7] eV appears in the insulating phase [12]. **Figure.I-4** illustrates this VO_2 band transition.

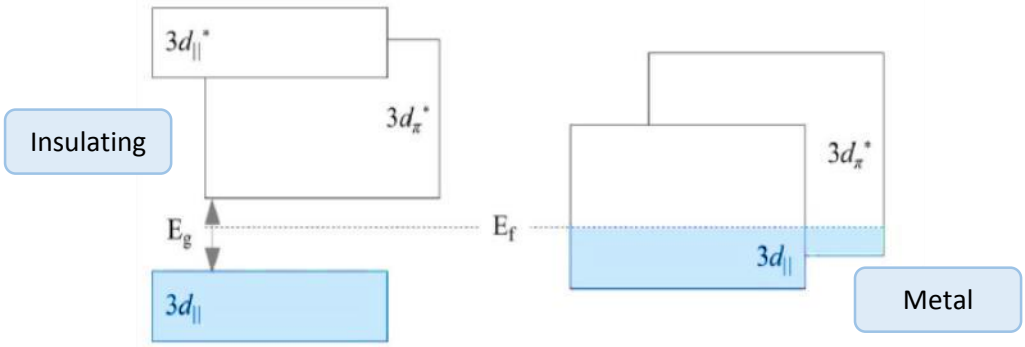

Fig.I-4: VO_2 band structure representing the insulating-metal transition [19].

d. Electrical and optical properties

As a result of the change in band structure and structural transition, the insulating-to-metal transition of vanadium dioxide is accompanied by a significant change in its electrical and optical properties. Indeed, the electrical resistivity decreases by 3 to 5 orders of magnitude between the two states depending on the quality of the material (up to five orders of magnitude for a single crystal [13], [9]). The following figure (**Figure.I-5**) shows the resistivity of VO_2 as a function of temperature compared to other materials with an insulating-to-metal transition.

As can be seen, the two conductivity measurement curves for temperature rise and fall do not overlap, thus forming a hysteresis cycle. In addition, vanadium dioxide is transparent at low temperatures in the infrared microwave range and becomes opaque and reflective at high temperatures in the same wavelength range (**Figure.I-6**).

As we will see later, in the case of thin films, the nature and orientation of the substrate and deposition conditions play an important role in the transition quality of VO_2 and the width of hysteresis. Several studies of the effect of substrate type and orientation have been conducted on Sapphire substrates, Si, SiO_2 [14], MgO [15], TiO_2 [16] and many others. Deposited on the same type of substrate, the deposition presents a transition

that naturally depends on the crystallographic orientation of the substrate, since it often imposes the orientation of the film [17].

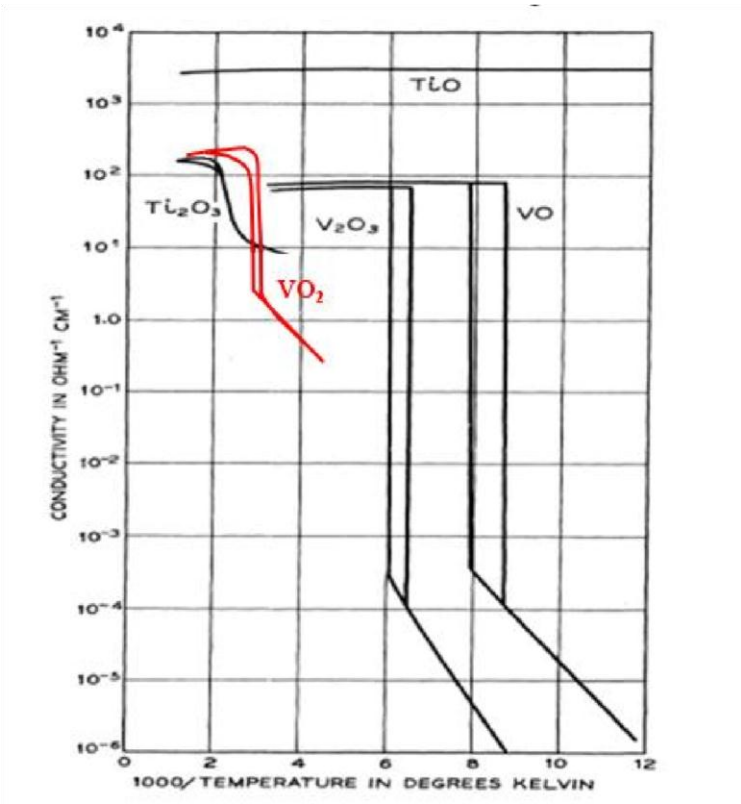

Fig.I-5: Electrical transition properties of single crystal VO_2 compared to other oxides [9].

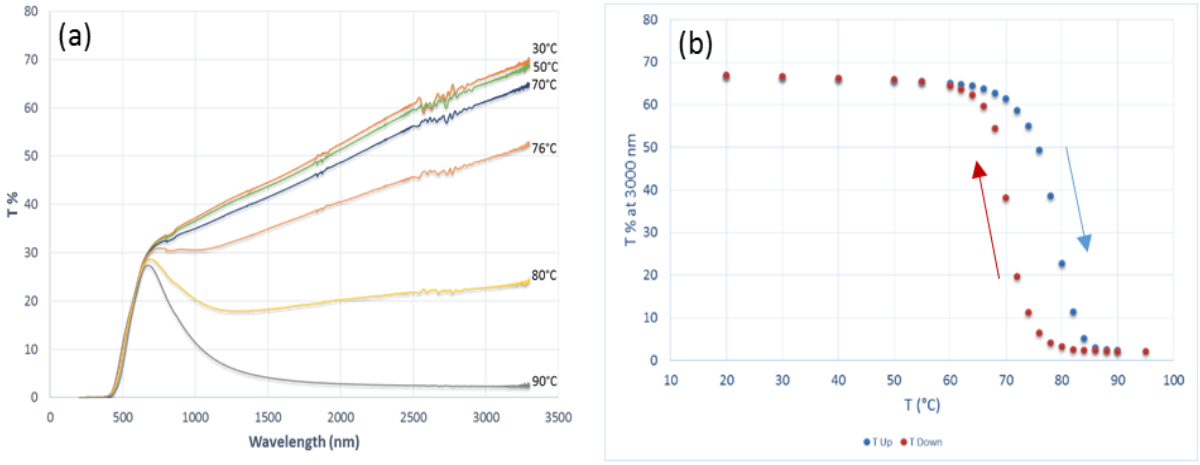

Fig.I-6: Optical transmission of VO_2 (a) at different temperatures and wavelengths and (b) at 3000 nm during heating and cooling.

There are many other V−O binary compounds with unique properties beyond the most used ones. A complete guide to the various V=O phases can be found in Ref. [20], including a diagram that represents the different V−O oxide phases as a function of their oxygen atomic fraction, obtained by thermodynamic calculations.

I.4 Phase transitions in vanadium oxides

A number of simple oxides of transition elements have a variation of their electrical resistance as a function of temperature; this is the case of several vanadium oxides that have been the subject of intense research, on this property in recent years. The latter are undergoing a state transition semiconductor to metal at critical transition temperatures (Tc) that vary from an Oxidizes to each other. The most extraordinary being VO_2 with a transition temperature close to the ambient temperature is 341°K (68°C). In comparison, VO has a Tc of -147°C, $V_2O_3$of -133°C and V_2O_5 of 250°C [21].

I.4.1 In vanadium dioxide VO_2

Vanadium dioxide undergoes a reversible phase transition (Tc = 68°C), its monoclinic form will be transformed into a quadratic form of rutile type structure. This transition is reversible and modifies the properties optical and electrical properties of the material, these modifications result from a transition from a semiconductor type to a metallic state: the low temperature form being a semiconductor form while the high temperature form has metallic type properties.

Given this transition from semiconductor to metal phase, it can be demonstrated in several ways: the first concerns resistivity or electrical conductivity.

At a temperature below the transition temperature of VO_2 the resistivity is high, once the transition temperature has been exceeded the resistivity drops sharply and the metal phase is obtained. What we observe in heating, we can find it again when cooling the material with however a slight hysteresis, i.e. a non-reversible variation in terms of temperature for the phase change.

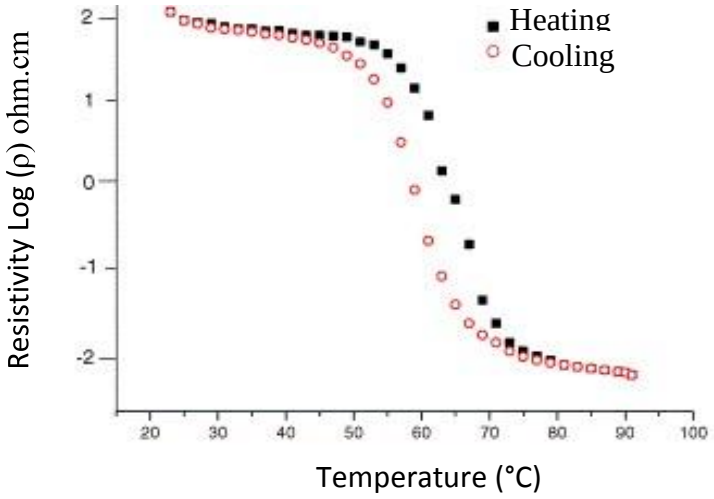

Fig.I-7: Variation of electrical resistivity as a function of temperature [23].

What is actually of interest to thermochromic materials is their variation in optical properties. **Figure.I-8** shows the variation in the transmittance of the vanadium dioxide layer as a function of temperature at different wavelengths. It can be seen that in the visible range, the phase transition does not affect the overall optical properties of the material.

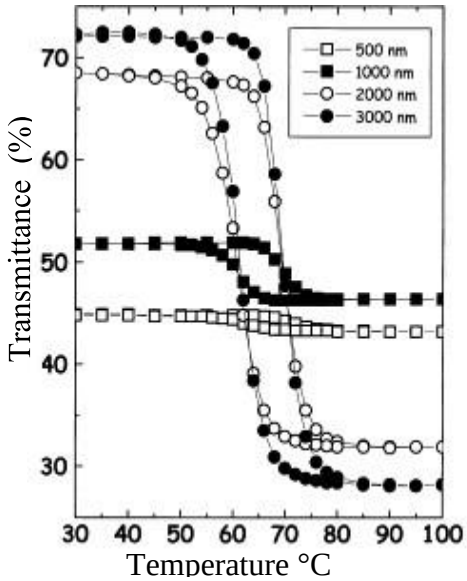

Figure.I-8: Variation of the transmittance of a VO_2 film as a function of temperature for different wavelengths [23].

On the other hand, the more we go towards the infrared, the greater the variation in the transmittance of the film becomes.

Whether on the electrical or optical properties of the material, the transition will always be accompanied by a hysteresis that will be more or less wide.

- **Influence of doping on vanadium dioxide phase transitions**

For some applications, it is essential to reduce or increase the transition temperature. For this there may be several solutions, the most important one being to boost vanadium dioxide with different elements. To date, a number of elements have been tested to modify this transition temperature.

The main elements that have been tested are tungsten, molybdenum and fluorine. These elements have the effect of reducing the transition temperature.

On the other hand, other elements such as tin or aluminium will tend to increase the transition temperature.

This property of being able to vary the transition temperature according to doping is very interesting for the applications that can result from it in the fields of thermal sensors.

- **Molybdenum-doped VO_2**

The electrical resistivity of the films decreases at a temperature higher than the transition temperature, which corresponds to the phase change of VO_2 from semiconductor to conductor.

The transition temperature of VO_2 thin films is 64°C for undoped layers and 41°C for doped layers.

It is clear that molybdenum doping reduces the transition temperature of thin layers of VO_2.

- **VO_2 doped with tungsten**

Figure.I-16 shows infrared transmittance spectra (λ = 2500 nm) of VO_2 layers doped with tungsten. It can be seen that, depending on the level of tungsten doping provided, it is possible to reduce the transition temperature to about 45°C for films doped with 0.9% tungsten atoms; we also see that tungsten doping will induce, in the case of a certain critical dose exceeded, a strong attenuation of the material's transmittance.

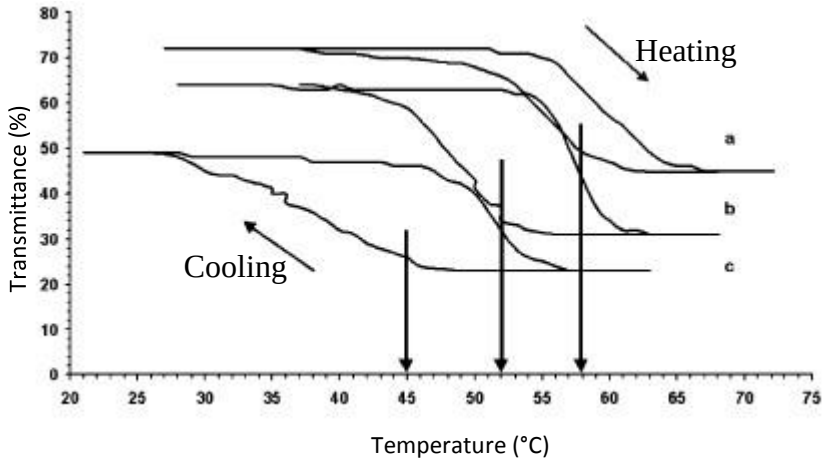

Fig.I-9: Hysteresis curves of the IR transmission at 2.5 µm for VO_2 thin films doped with different proportions of tungsten: (a) 0.3%, (b) 0.6% and (c) 0.9% [25].

I.4.2 In vanadium pentoxide V_2O_5

Vanadium pentoxide V_2O_5 undergoes a reversible and rapid transition from a semiconductor to a metal phase near 250°C [22]. For V_2O_5 thin films, the transition temperature depends on the technique and experimental conditions of the deposits used.

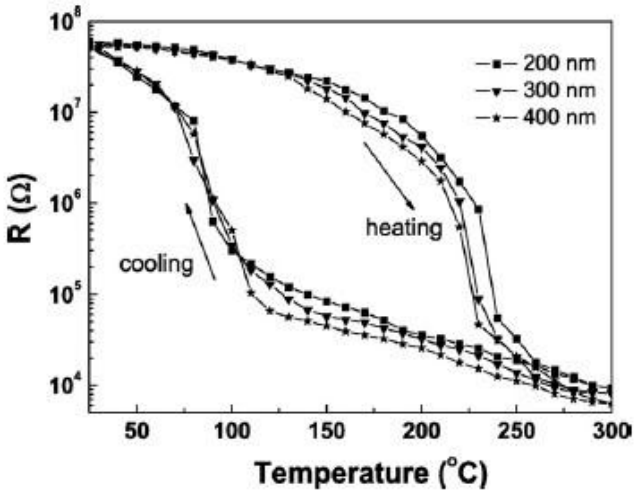

Fig.I-10: Variation of the resistance of V_2O_5 films of different thicknesses as a function of temperature [26].

Figure.I-10 shows the variation in the electrical resistance of V_2O_5 films of different thicknesses deposited by thermal evaporation as a function of the temperature of the heating.

We can clearly see a decrease in the electrical resistance of the thin layers of V_2O_5 from a critical temperature of about 230°C over the heating cycle. This decrease is the result of the transition from the semiconductor state to the metallic state of V_2O_5, which is reduced to 130°C during cooling.

Figure.I-11 shows the IR transmittance spectra of V_2O_5 films deposited with an oxygen partial pressure of 20% with different molybdenum dopant element (Mo) levels before and after heating to 200°C.

There is a greater trend in the variation of the transmission coefficient when the doping rate increases with a temperature of 200°C. The variation of the transmittance reached is 49% at λ= 4000 cm^{-1}. All these properties of V_2O_5 indicate that the thin layers of V_2O_5 have a good thermochromic behaviour in the wavelength range between 3600 and 4000 cm^{-1}. They are ideal thermochromic materials.

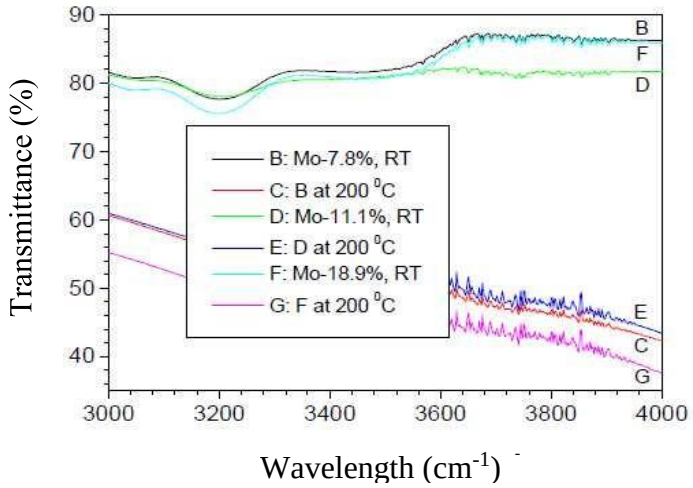

Fig.I-11: Infrared spectra of V_2O_5 films deposited with 20% PO_2 and different Mo dopant levels before and after a heating of 200°C [27].

I.5 VO_x for infrared applications

Of all the phases reported in the previous section, V_2O_5 and VO_2 are the most commonly used in bolometers. Their properties are discussed in more detail in this section. V_2O_5 has the highest level of oxidation with its $3d^0$ orbital and is the most stable phase of the system [28]. A rectangular grain structure (nano-sticks), as shown in **Figure.I-12**.

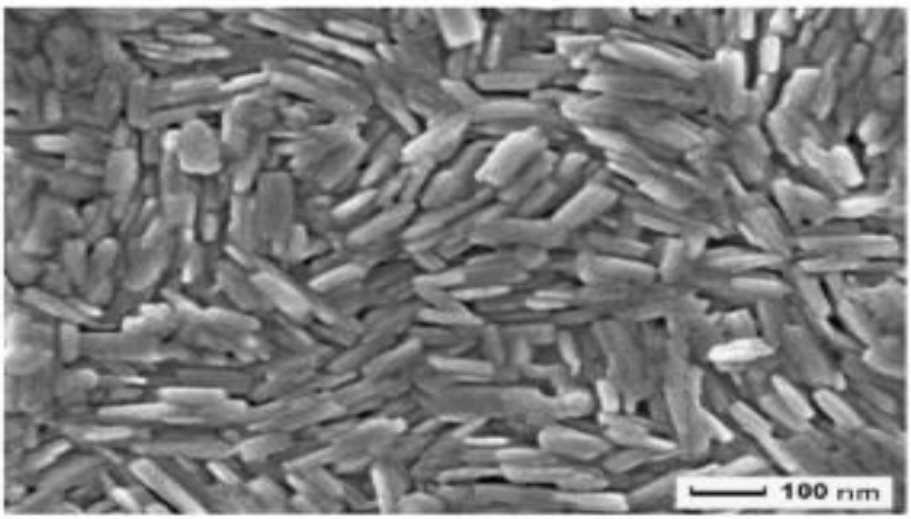

Fig.I-12: Nano stick structure of the V_2O_5 [29].

V_2O_5: Is a stack of sheets connected together by Van De Walls forces. This particular structure gives it many applications for ion storage and catalysis, especially for lithium batteries and gas detectors [30]. The low strength of the bond between the sheets allows molecules to be inserted between them or to dissociate them directly in water. However, this sensitivity to the aqueous medium is a disadvantage when using this material for bolometers, since the subsequent manufacturing steps of the device often require wet etching.

VO_2: The transition from metal to semiconductor of VO_2 at 68°C causes a change in resistance and transmittance. This gives it applications for smart windows, switches and optical memories [31]-[32]. The semiconductor configuration combines excellent TCR and bolometer resistivity. Although the transition is caused by mesh distortion, thin layers of VO_2 have been shown to be resistant to more than 10^8 cycles [33]. However, the resistance must vary linearly for infrared detection. The transition at 68°C therefore sets an upper temperature limit to the conditions of use of this phase for this application.

I.6 Conclusion

The fascinating properties and broad applications of vanadium oxide, particularly in the form of thin films, have attracted considerable interest. Multivalent, layered structure...They can be used as a catalyst, gas sensor, as an optical window in photovoltaic solar cells.

Chapter II

Thin Films: Generalities

II.1 Introduction

The ever-increasing integration of devices, especially in the field of microelectronics, requires the development of increasingly sophisticated deposition techniques for the elaboration of materials in the form of thin layers. After a presentation of definitions and mechanisms of formation of thin films, we focus on some of the most used methods to obtain VO_X oxide in the form of thin layers.

II.2 Definition of thin layer

In principle, a thin layer of a given material is an element of this material of which one of the dimensions called thickness has been greatly reduced so that it is expressed in Angstrom and this short distance between the two boundary surfaces (this quasi two-dimensional) causes a disruption of most of the physical properties [34]. The essential difference between the material in the massive state and in the state of thin layers is related to the fact that in the massive state the role of the limits in the properties is usually neglected with reason, whereas in a thin layer these are on the contrary, the effects related to the major surfaces that are preponderant. It is obvious that the lower the thickness, the more this two-dimensional effect will be important, and that when the thickness of a thin layer exceeds a certain threshold, the effect of thickness will become minimal and the material will recover the properties well. Known from the massive material.

The interest of thin films comes mainly from the economic use of materials in relation to the physical properties and the simplicity of the technologies implemented for their realization. A wide variety of materials is used to produce these thin layers. These include metals, alloys, refractory compounds (oxides, nitrides, and carbides), intermetallic compounds and polymers.

The second essential characteristic of a thin layer is, whatever the procedure used for its manufacture, a thin layer is always integral with a support on which it is deposited (although it sometimes happens that the film is separated. thin of said support).

Consequently, it will be imperative to take into account this major fact in the design, namely that the support has a very strong influence on the structural properties of the layer deposited therein. Thus, a thin layer of the same material, of the same thickness may have substantially different physical properties depending on whether it will be deposited on an amorphous insulating substrate such as glass, or a monocrystalline silicon substrate, for example. These two essential characteristics of a thin layer result in the following consequence: a thin layer is anisotropic by construction.

In practice we can distinguish two main families of methods, those that use a carrier gas to move the material to be deposited from a container to the substrate and which are similar to the diffusion techniques used in the manufacture of active components, and those that which involve a very low pressure environment and in which the material to be deposited will be conveyed by means of an initial pulse of a thermal or mechanical nature.

II.3 Thin film formation mechanism

Thin film formation is achieved by a combination of nucleation and growth processes, described as follows [35]:

- Species, at the time of impact on the substrate, lose their travel speed component and are physically absorbed on the surface of the substrate. This is only true if the energy of these species is not too high.
- Initially, the absorbed species are not in thermal equilibrium with the substrate, and therefore move on its surface. During these movements, they will interact with each other; creating clusters that will develop.
- These clusters, called islets or nuclei, are thermodynamically unstable and naturally tend to desorb. However, if the deposition parameters are such that the islets collide with each other, it develops dimensionally. When they reach a certain size, the islets become thermodynamically stable. It is said that the nucleation threshold has been crossed. This stage, which sees the formation of stable, chemically absorbed islets of sufficient size, is called nucleation.

- The islets continue to grow in number and size until a nucleation density called saturation is reached. The nucleation density and the average size of the islets depend on several parameters such as the energy of the incident species, their quantity per unit time and area, the activation, absorption, desorption, thermal diffusion, temperature, topology and chemical nature of the substrate. An islet can grow parallel to the substrate surface by surface diffusion of absorbed spaces or perpendicular by direct impact of incident species on the islet. In general, the lateral growth rate is much higher than the perpendicular growth rate.

-The next step in the thin film formation process is called coalescence. The islands begin to agglomerate with each other by reducing the surface area of the uncoated substrate. Coalescence can be accelerated by increasing the surface mobility of adsorbed species, for example by increasing the temperature of the substrate. During this step, we can observe the formation of new islets on surfaces freed by the rapprochement of older islets.

- The islets become islands that continue to grow, leaving only small holes or channels between them. The structure of the layer changes from discontinuous to porous. Gradually, a layer continues to form as the holes and channels fill.

- So we can summarize the process of growth of a thin layer by saying that it is a statistical sequence of nucleation, then growth by surface diffusion and islet formation, then formation of larger islands, and finally the formation of a continuous layer by filling species between these islands. Depending on the thermodynamic parameters of the deposition and substrate surface, the islet nucleation and growth steps can be described as:

- **Of the island type (called Volmer-Weber):**

During three-dimensional (3D) growth, or Volmer-Weber growth, small germs are formed on the surface of the substrate. These grow to form islets that then coalesce to form a continuous thin layer. This growth pattern is usually favored when the atoms forming the deposited layer are more strongly bonded to each other than to the substrate, as is the case for the growth of metals on insulators or contaminated substrates.

- **Of the layer type (called Frank-van der Merwe):**

Two-dimensional (2D) layer-bylayer growth, or Frank-van der Merwe growth, is promoted when the binding energy between the deposited atoms is less than or equal to that between the thin layer and the substrate. In addition to homoepitaxial growth, there are many examples in hetero-epitaxy of semiconductors (e.g. GaAlAs/GaAs) and metals (e.g. Cd/W).

- **Of the mixed type (called Stransky-Krastanov):**

The third growth mode, called Stransky-Krastanov (SK), is a combination of the two previous modes: after a two-dimensional growth start, we observe a change in growth mode as the formation of islets becomes energetically favourable. This transition from 2D to 3D growth mode is not yet fully understood, although it can be induced by the relaxation of the elastic energy stored in a constrained heterostructure. This phenomenon is at the origin of the formation of self-organized structures and undulations in structures with compensated stresses.

Figure.II-1 shows the three types of thin film formation. In fact, in almost all practical cases, the growth of the layer is achieved by the formation of islets, then islands, then a continuous surface. Except in the case of special deposition conditions (substrate temperature, nature and energy of incident species, chemical nature of the substrate, ambient gas characteristics...), crystallographic orientations and topographical details of islets are randomly distributed. This means that, when these islets meet during the growth process, various grain joints, defects and dislocations will be included in the layer as a result of geometric configuration and crystallographic orientation disagreements [35].

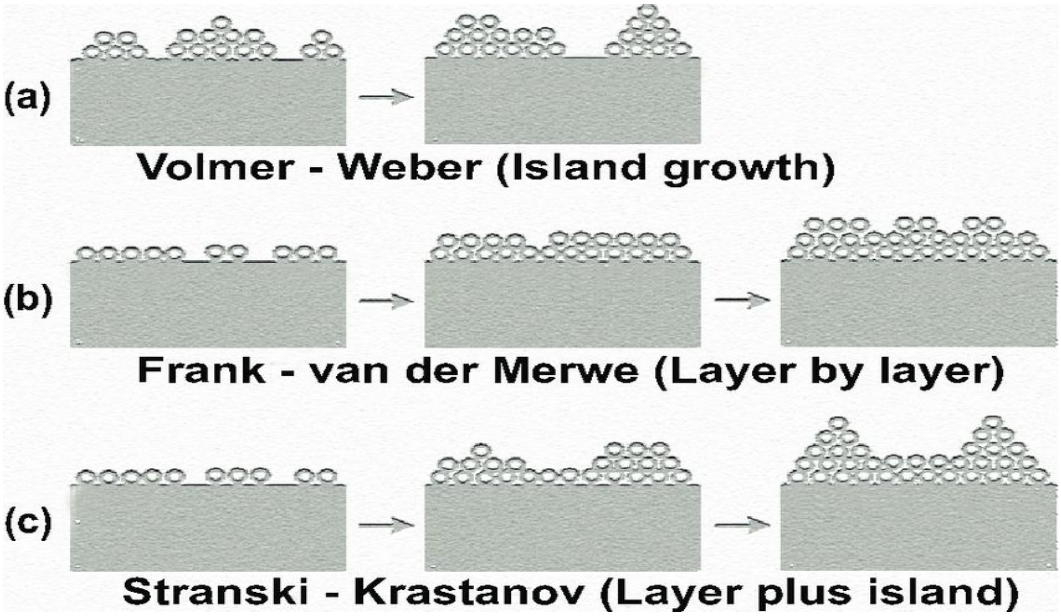

Fig.II-1: The three main growth modes of thin films [36].

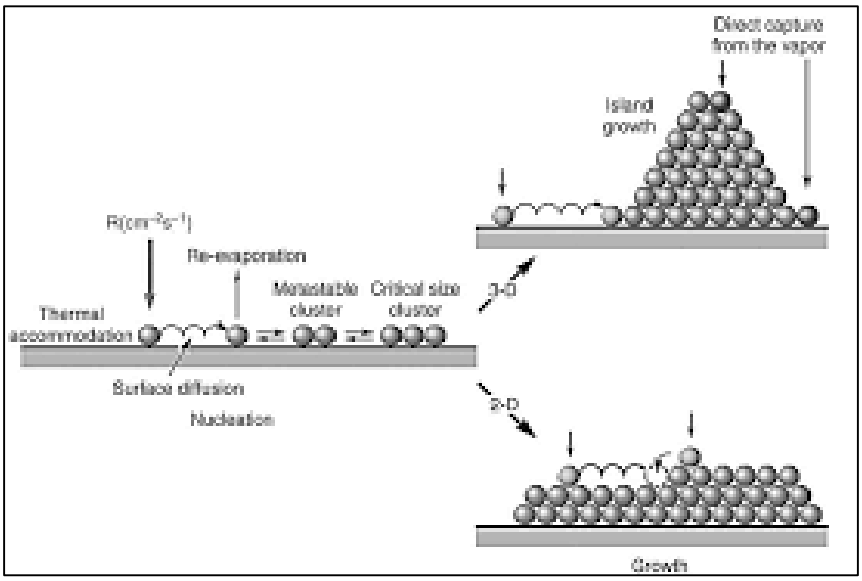

Fig.II-2: The growth modes of a thin film according to the kinetic process [37].

If the grains are randomly oriented, the layers will be said polycrystalline. However, if the grain size is very small (around 20°A), the layers will have amorphous (non-crystalline) structures. It should be noted that, although the orientation of the different islets is the same over the entire surface of the substrate (which can be obtained by special deposition conditions) and that this substrate is a single crystal, would not obtain a monocrystalline layer. In this case, the layer will be made of grains monocrystalline oriented parallel to each other and connected by joints of low angle grains. These layers are called epitaxial monocrystalline.

Other causes that can cause defects in thin films include [34]

- A very large difference in the mesh parameters between the layer and the substrate.
- The presence of significant stresses in the layer.
- The extension in the layer of dislocations present on the surface of the substrate.

After a continuous layer is formed, anisotropic growth occurs perpendicular to the substrate surface in the form of cylindrical columns. The diameter of these columns is mainly determined by the initial nucleation density.

However, if recrystallizations occur during the coalescence phase, the average amount of grains per unit area of the layer will be lower than the initial nucleation density. For layers with a thickness of less than one micron, the perpendicular dimension on the surface of the grains will be practically equal to the thickness of the layer. For diapers thicker, a nucleation occurs on the surface of the grains and each vertical column will grow in a multigranular way, with possible deviations from growth perpendicular.

Agglomeration effect

Agglomeration is driven by the high surface to volume ratio of thin films. Surface diffusivity, which is exponentially dependent on temperature, acts to reduce the surface area through capillarity. The process is a nucleation and growth process. Defects, pinholes or thermal grooving at a grain boundary must first establish a hole greater that

a critical radius, which is determined by the film thickness and wetting angle. Stress can hasten the formation of a hole by differentially thinning the material. Once the critical radius is achieved, the hole will grow until the film is transformed into a collection of unconnected, hemispherical islands which are electrically isolated.

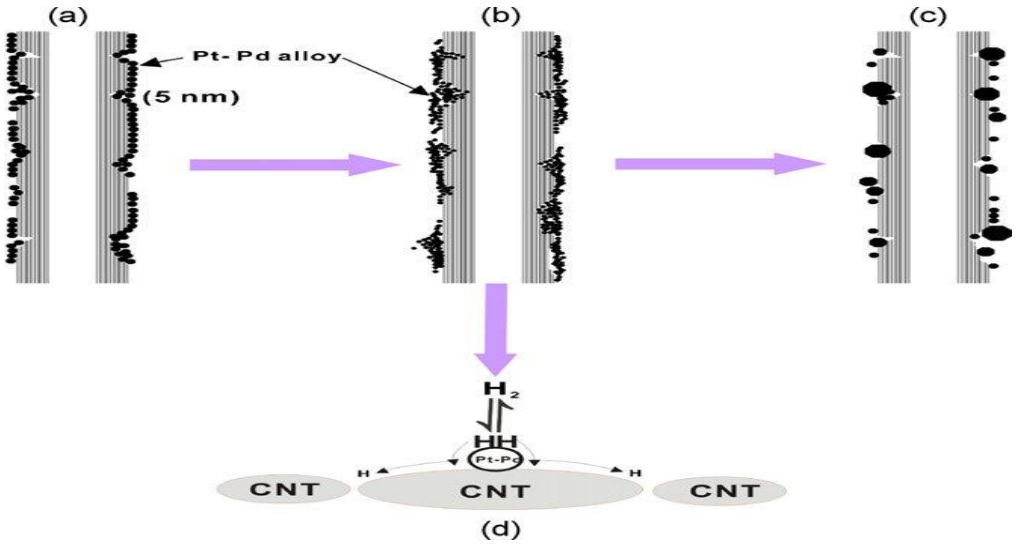

Figure.II-3: Schematic diagram of agglomeration of metal nanoparticles during the hydrogenation cycles. (a) Corresponds to the Pt-Pd coated carbon nanotubes before hydrogenation, (b) during hydrogenation, and (c) after successive number of adsorption/re-adsorption cycles. (d) Spillover of atomic hydrogen dissociated by the platinum-palladium alloy nanoparticles to the pristine carbon nanotube.

- **Vanadium oxidation**

The oxidation of vanadium in an oxygen atmosphere leads to the formation of a compact oxide layer containing mainly V_2O_5 but also the sub-oxides V_6O_{13}, V_3O_7 and VO_2; simultaneously the metal dissolves a small amount of oxygen with formation of the VO_x phase. For flat and thin samples, oxidation is initially governed by a mixed diffusion regime sensitive to pressure in the oxidized layer and metal. After saturation of the substrate, the volume diffusion regime both cationic and anionic that is established through the oxide coating is independent of the oxygen pressure.

II.4 Thin film deposition procedure

All thin film deposition processes contain four (sometimes five) successive steps. The source, which constitutes the basic material of the thin film to be elaborated, may be a solid, a liquid, a vapor or a gas. When the material is solid, it is transported to the substrate by vaporization. This can be achieved by thermal evaporation, electron gun, laser ablation or by positive " spray " ions. All of these methods are classified under the name PVD physical vapor deposition. The solid source is occasionally converted to vapor chemically. In other cases, the base material is in the form of a gas or liquid having sufficient vapor pressure to be transported at moderate temperatures. Processes that use gaseous, evaporated or chemically evaporated liquids as base material are known as chemical vapor deposition, i.e. CVD "Chemical vapor deposition" [38].

In the transport stage, the uniformity of the flow of the species arriving on the surface of the substrate is an important element; several factors can affect this uniformity and depend on the medium in which the transport takes place, a high vacuum or a fluid "mainly gases". In the case of a high vacuum, the molecules, coming from the source and going towards the substrate, cross the medium in straight lines, whereas in a fluid medium they undergo several collisions during their transport. Consequently, in a vacuum, the uniformity of the flux that arrives on the substrate is determined by the geometry, whereas in a fluid it is determined by the flow of the gas and by the diffusion of the molecules of the source in the other gases present. . Often, processes that use high vacuum are equivalent to PVD processes while those that use a fluid flow are CVD methods. This definition is not always confirmed. There are several physical vapor deposition processes operating in a high vacuum, others such as laser ablation and sputtering often operate at high characteristic fluid pressures. Similarly, the majority of CVD deposition processes are found to operate at moderate pressures, while chemical beam epitaxy. Epitaxy operates in a vacuum.

In this phase, several thin film deposition processes use a plasma medium. Indeed, the large amount of energy contained in this medium allows, at low temperature,

the activation of the formation of the layers. The working pressure of a plasma can be that of a fluid or that of a high vacuum. The third step in the processes for producing thin films is the deposition of the film on the surface of the substrate. The deposition process is determined by source factors, transport and also by the three main conditions of the substrate surface. The latter are the surface state "roughness, level of contamination, degree of chemical bond with the incoming material", the reactivity of the material arriving on this surface "Sticking coefficient" and the energy deposited on the surface "Substrate temperature, Photons, positive ions ". The last step in the manufacturing process is the need for analysis of the resulting film. The first level of material control is to make direct measurements of its important properties. If the results of the analysis are insufficient, it is essential to resort to particular experiments that make it possible to remove the possible ambiguities of a given process.

II.5 Thin film deposition methods of V_XO_Y

The thin layers of vanadium oxide are made using a wide variety of techniques due to the variety of applications of this material. They can be obtained by operating in the liquid phase or in the vapor phase, and by physical or chemical processes.

By liquid means, the most frequent techniques are: chemical deposition in solution [39], electro-deposition by electrochemical synthesis [40] and sol-gel route [41]. By vapor, we distinguish physical methods "PVD" chemical methods "CVD". As part of this thesis, we will first present some techniques using the steam path while reserving a more in - depth development to thermal evaporation, a technique that has been chosen for this work.

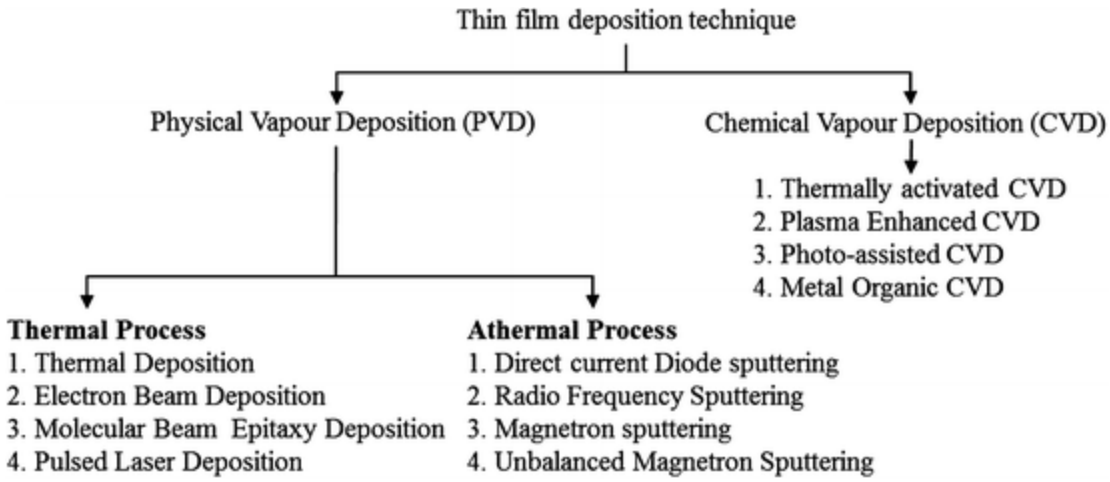

Figure.II-4 : Thin films deposition technique [42].

II.5.1. Chemical vapour deposition

CVD methods make it possible to produce deposits from gaseous precursors that react chemically to form a solid film deposited on a substrate. The most used synthetic methods are:

- The decomposition deposition of organometallic compounds (MOCVD) either at atmospheric pressure [42] or at low pressure [43];
- Deposition by pyrolysis of aerosol, also called "spray pyrolysis" from aqueous solutions; this technique is widely used especially for oxides because the deposits are produced under a normal atmosphere [44, 45];
- Deposition by atomic layer (ALD) [46] or epitaxial (ALE) [47] and photo-ALE [48].
- Plasma enhanced chemical vapor deposition (PECVD) [49], photo-CVD [50].

The main advantages of these techniques are to allow the crystallization of films without resorting to annealing, to be able to control the composition during the deposition, to produce a deposit of uniform thickness and composition, which has excellent adhesion. However, these techniques have the disadvantage of giving films contaminated by the residues of the precursors and that of having an often high reaction temperature.

II.5.2. Physical vapor deposition

PVD processes mainly include evaporation, laser ablation and spraying in all its forms. In making a layer, the following three steps can be distinguished:

- The creation of the species to deposit, in the form of atoms, molecules or clusters (groups of atoms or molecules).
- The transport of these species in the vapor phase from the source to the substrate.
- The deposit on the substrate and the growth of the layer.

a. Pulsed Laser Deposition

PLD (Pulsed Laser Deposition) consists in focusing a laser beam on a material in order to vaporize it and then to condense the ionized particles on a heated substrate or not. It should be noted that the ionized particles have a high kinetic energy (a few tens of electronvolts).

Deposition of thin films of VO_X by PLD has the advantage of being able to use high oxygen pressures and of making high quality crystalline films with a high growth rate even at low temperatures [51]. The microstructure, the crystallinity, the orientation and the optical properties of the VO_X layers are all the better as the oxygen pressure is important. Increasing pressure can reduce defects such as oxygen deficiency [52].

Matsubara et al [53] have shown that conductivity and optical transmission increase with oxygen partial pressure. This is due to the increase in the molecular reactivity of the oxygen gas incorporated in the VO_X layers. The deposits made by this technique have better crystallinity and structural and optical properties. This is due to the decrease in defects and the increase in grain size [54].

Laser ablation, however, has limitations due to the unreliability of lasers, and its high cost. This benefits other techniques easier to use such as sputtering that we will present below.

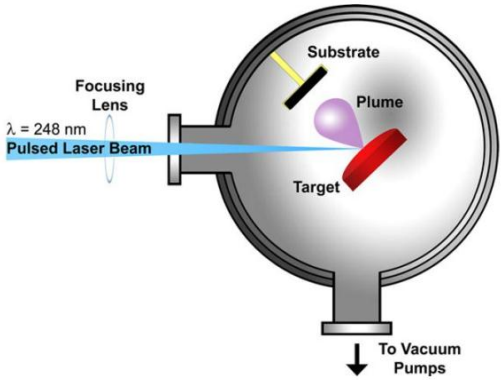

Figure.II-5: A schematic for a typical experimental arrangement for the pulsed laser deposition technique [55].

b. Sputtering

In this method, the substrate is placed in a chamber containing a gas (usually Argon) at low pressure, in which an electric discharge is caused. This discharge has the role of ionizing the gas atoms. The ions thus obtained are accelerated by a potential difference and come to bombard a cathode made up of the material to be deposited [55, 56]. Under the impact of accelerated ions, atoms are torn off the cathode and deposited on the substrate. In some cases, a gas is introduced into the chamber in addition to argon, which will react chemically with the atomized atoms to form the material that it is desired to obtain. Then, we have a reactive cathode sputtering. This method allows for low resistivity deposits and good stoichiometry with average visible transmission [57].

The advantage of the sputtering method is that it can produce deposits under controlled atmospheres. However, the high cost of the installation, associated with a low production rate makes sputtering a technique reserved for specific applications reduced. The choice of a particular thin film deposition technique depends on several factors [58]. We mention the material to be deposited, the desired deposition rate, the limits imposed by the substrate, such as the maximum deposition temperature, adhesion of the deposit on the substrate, the deposition on complex substrates or not, the purity of the material envisaged for the ideal solution and for an alternative solution, the ecological considerations and the ease of supply of the material to be deposited, in the present and the future.

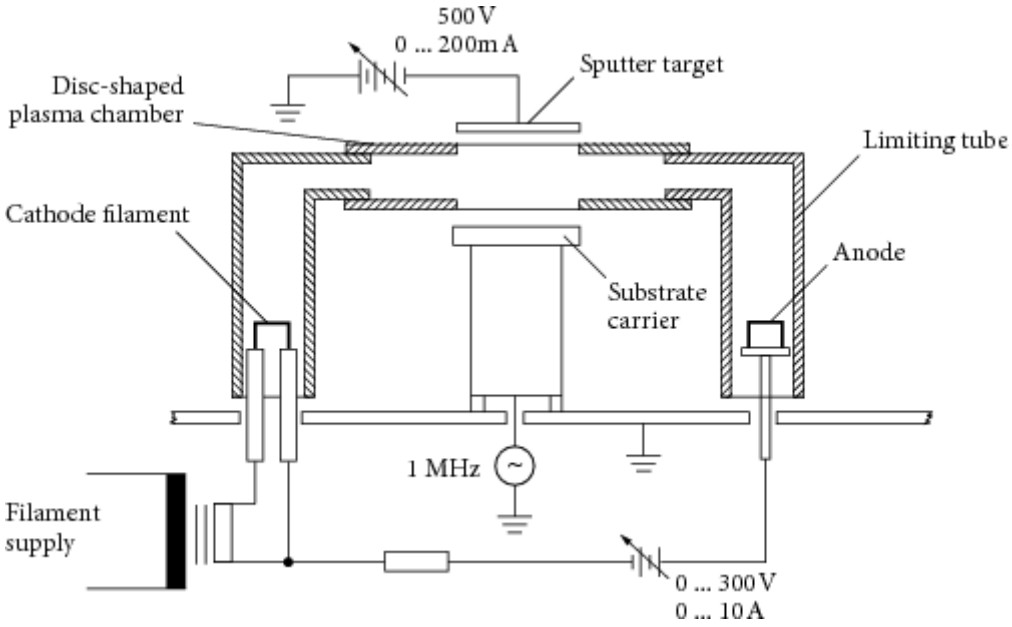

Fig.II-6: Cathode sputtering technique [58].

c. Vacuum evaporation

The vapours of the material to be deposited are obtained by heating it by various means: Joule effect, induction (coupling of a high frequency generator), electron gun, laser beam or electric arc. The evaporation is carried out under a high vacuum (pressure of the order of 10^{-3} to 10^{-4} Pa) [59] in order to increase its speed.

As the vapor flow is localized and directional, it is often necessary to print on the substrate a rotational or translational movement with respect to the evaporation source, so as to achieve homogeneous deposition and uniform thickness. The best results are obtained on surfaces practically perpendicular to the vapor flow [60]. When the pressure is not sufficiently low the deposits are not very adherent and often amorphous.

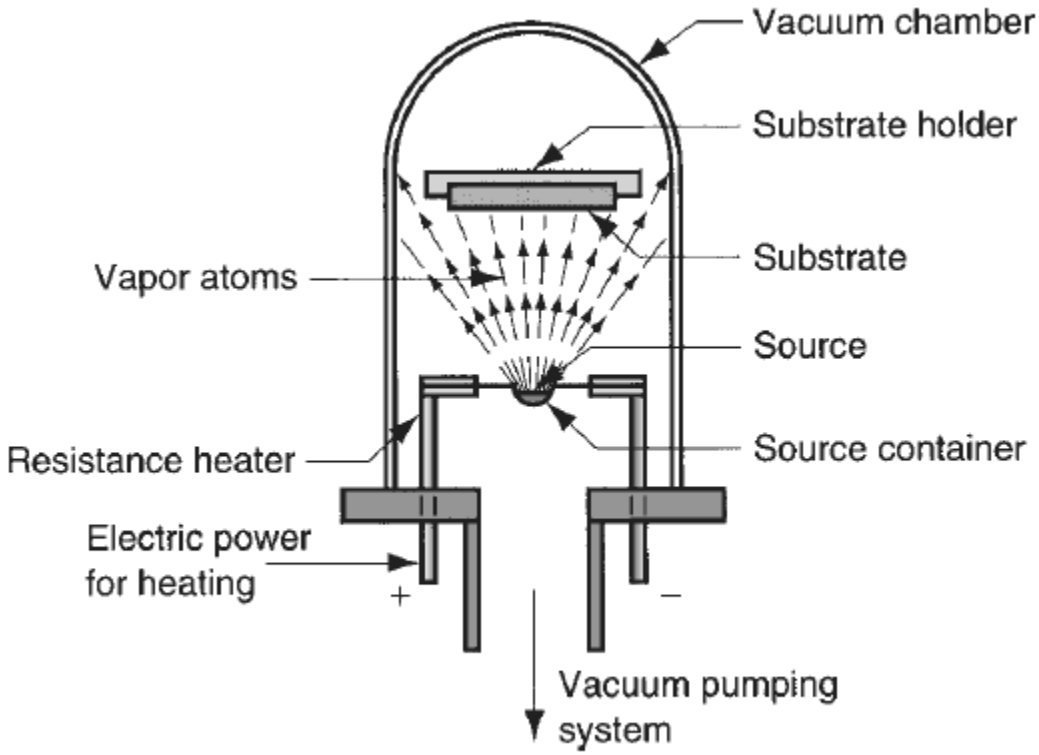

Figure.II-7: Vacuum chamber Evaporation [61].

In general, the main problems encountered during evaporation are:

- ✓ The dissociation of the oxides.
- ✓ The reaction of the materials to be evaporated with those with which they are in contact.
- ✓ Degassing, decomposition, micro-explosions of materials to evaporate.
- ✓ The difficulty of obtaining layers of alloys having the same composition as the starting alloy.

Evaporation remains however a particularly appreciated method because one thus elaborates very pure materials and even more pure that the pressure is weak, which is the case for the method of molecular beam epitaxy [61, 62]. However, it is not suitable for the production of thermodynamic equilibrium films.

Different thin layers of doped VOx have been successfully prepared by evaporation under vacuum [63, 64]. The thin films of VOx studied in the context of this work were carried out using the vacuum evaporation method which will be described in the following **chapter III**.

- **Bibliographic review on thermal evaporation technique**

The fabrication of thin films of VO_x by thermal evaporation process is an old research topic, which remains very active as attested by the number of publications on the subject, most of these publications are for V_2O_5 synthesis [65], [66], [67], [68].

We will analyse these articles in diachronic order of their publication.

Granqvist et al [68] have succeeded to made thin vanadium oxide films by vacuum evaporation in order to study the evolution of thermochromism when vanadium films are oxidized in air. The aim is to elucidate the conditions in which VO_2 films-of considerable potential interest for energy-efficient window -are formed.

On 2007 [66] Davinder Kaur and his co-authors have grown V_2O_5 thin films on amorphous glass substrates using vacuum evaporation technique and have studied their structural and optical properties. They have found that the films grown at room temperature were homogeneous, uniform and smooth texture but are amorphous in nature which could play an important role as a cathode in fabrication of thin films batteries. The best quality films grown at deposition temperature of 300°C are well textured and c-axis oriented with good crystalline properties. Deposition temperature was found to have a great impact on the optical and structural properties of these films.

The observed decrease in lattice constant with increase in deposition temperature is attributed to the oxygen loss in V_2O_5 structure, which usually leads to contraction of (001) interplanar spacing. AFM analysis shows that with increase in deposition temperature both the surface roughness and the grain size increase

Recently on 2013 [65], J.P.veiga et al reported the deposition of vanadium oxide films by thermal evaporation in order to study thermoelectric proprieties of V_2O_5 thin films; as a result they said that the as-deposited V_2O_5 thin films produced by thermal evaporation technique without intentional substrate heating present an amorphous structure. After thermal treatment at temperatures around 675°K for 1h at atmospheric environment conditions the films show a predominant (0 0 1) plane reflection of the orthorhombic V_2O_5 phase ($2\theta = 20°$C). Furthermore, the films crystallinity increases as T of annealing increases. The XRD analysis has been further substantiated by SEM and AFM analysis, revealing an increase in surface heterogeneity and roughness, respectively. The electrical conductivity of the V_2O_5 films is also strongly influenced by the annealing.

More recently 2018 [67] Luis Henrique Cardozo Amorina et al have use resistive thermal evaporation under high vacuum in an HHV (AUTO306) system to deposit vanadium oxide, because it offers a better control to the thin film composition, and structural and morphological aspects The aim of the work was an investigation on the influence of the morphological properties, crystallite size and roughness as thickness dependent, on the reversible specific charge capacity and the respective optical responses. The samples were thermally treated in an oxidizing atmosphere (O_2) at 400 ºC by 2hours. It was found that by increasing of the film thickness from 50 to 160 nm, the morphology of the film became more uniform, reducing its surface roughness.

II.6 Deposition of vanadium oxide films by thermal evaporation

A typical process to deposit vanadium oxide films by TE usually consists of two steps. The first step is to prepare a vanadium-rich metallic film or VO_x film. The target (typically metallic vanadium, VO_2, V_2O_5) is placed in a heated crucible made of Mo or W, located under the substrate in a high vacuum chamber (2.7–6.7 x 10^{-3} Pa).

II.7 The phenomenon of condensation

In theory, condensation is only possible when the substrate is colder than the emitting source. This condensation is still only possible below a critical substrate temperature that depends on the incident vapour flow. Indeed, the deposited atoms have a lifetime on the surface of the substrate after which they will be re-evaporated. When this lifetime is sufficient to allow other atoms to condense, the energy required to re-evaporate these funds increases. Growth then begins around the first nuclei of atoms and improves as the evaporation lasts. Nevertheless, the condensation process depends on several physical parameters associated with the manufacturing method.

II.7.1 Effect of pressure

As a general rule, according to the pressure-temperature diagram of stable materials, the melting point moves to low temperatures as the pressure decreases; this allows the volatilization of high melting point bodies that are difficult to reach at ordinary pressure. According to Holland [34], oxides and stable compounds begin to evaporate as soon as the vapour pressure reaches 10^{-2} mm Hg.

On the other hand, the pressure is directly related to the average free flow of steam molecules within the residual gases. The kinetic theory of gases shows that: if N_0 is the number of steam molecules from the crucible, **L** is their average free path in the residual gas, only **N** of they can cross a distance l without collisions with ambient gas molecules [69]; **N**, $\mathbf{N_0}$, $\boldsymbol{l}$ and **L** are then linked by the relationship:

$$N = N_0 e\left(\frac{-l}{L}\right) \quad \text{(II.1)}$$

It should be noted that pressure plays a very large role in the contamination of the deposit. In the case where the crucible is made of tungsten, it reacts at high temperature with dry oxygen to give a volatile oxide WO_3. According to Langmuir [70], at 1000°C, 0.1% of this oxygen reacts with tungsten, while at 1500°C; this proportion is multiplied by 25. In our films we have noticed the presence of W whose origin is the oxygen of WO_3.

II.7.2 The position

It is sufficient to recall the formula deduced from the kinetic theory of gases (formula II-1). It is then obvious that the larger the l, the lower the flow of atoms arriving at the substrate without collisions. On the other hand, the physical properties of the deposits are a function of the position of the substrate. It is useful to estimate the error introduced by the deviation of the position of the substrate from the vertical of the source

(Figure II.7) if we consider evaporation to a parallel plane substrate, the thickness of the deposition is given [76].

(a) From a point source by:

$$d = \frac{m}{4\rho r}\frac{cosq}{r^2} = \frac{mh}{4\rho r r^2} = \frac{mh}{4\rho r(h^2+d^2)^{3/2}} \quad \text{(II.2)}$$

If we call d^0 the thickness of the layer at the perpendicular lowered from the source to the substrate, we have:

$$\frac{d}{d_0} = \frac{1}{\left[1+(d/h)^2\right]^{3/2}} \quad \text{(II.3)}$$

(b) From a planar source by:

$$d = \frac{m}{\rho r}\frac{cos^2 q}{r^2} = \frac{mh^2}{\rho r(h^2+d^2)^2} \quad \text{(II.4)}$$

$$\frac{d}{d_0} = \frac{1}{\left[1+(d/h)^2\right]^2} \quad \text{(II.5)}$$

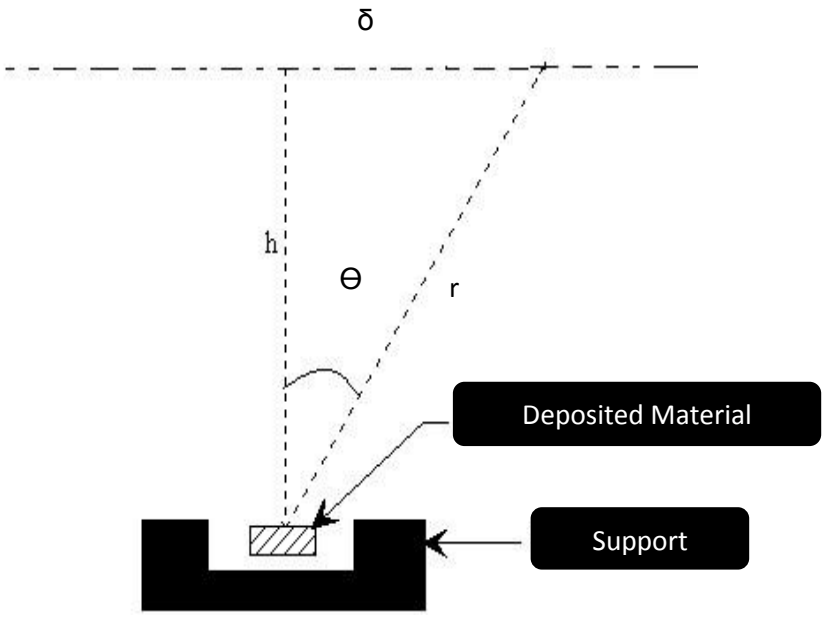

Fig.II-8: The deviation of the substrate position from the vertical of the source [77].

Figure.II-9 compares the two results obtained in the previous two years.

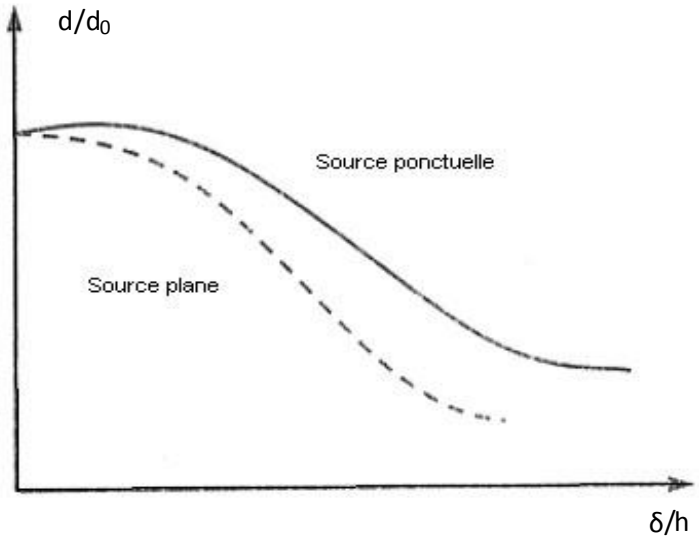

Fig.II-9: The thickness error introduced by the deviation of the substrate position from the vertical of the source [78].

II.8 Conclusion

In this chapter, we have presented general concepts on thin films. We made a general presentation on deposition techniques while focusing on the growth patterns of these layers.

Chapter III

Experimental procedure

III.1 Introduction:

The development of science and technology has improved many ways of thin film deposition technique over the time. Among that, one of the most basic and primitive process includes evaporation.

Let's say, a mechanism for the deposition of a very thin film of a material over a substrate (glass) is needed. This chapter will present a study on the experimental conditions for the development of thin layers of vanadium oxide by thermal evaporation and the different characterization techniques used for the study of the electrical and structural properties of thin films.

III.2 Thermal Evaporation Deposition System

During this study, the V_xO_y layers were developed from a rapid evaporation (at high temperature and very low pressure) of a V_2O_5 powder. The evaporator used during our experiments is a device mounted locally at the Advanced Technology Development Centre (CDTA). There is a cylindrical Pyrex glass enclosure with a volume of 7219 cm^3, this enclosure is closed from above by a 23cm diameter steel flange which contains air leaks and gas inlets. The device is equipped with a pumping unit that provides a high vacuum in the range of 10^{-6} mbar (**Figure.III-1**). The latter consists of a vane pump for the primary vacuum of about 1. 10^{-2} mbar and oil diffusion pump for the secondary vacuum. The materials to be deposited are placed in a tungsten crucible, which connects two electrodes which are in turn supplied through a transformer which rises to the current by an electric Variac (see **Figure.III-1**). The substrates are placed in a mobile substrate holder that is located in front of the crucible at a distance of 11cm, where up to 12 samples can be placed.

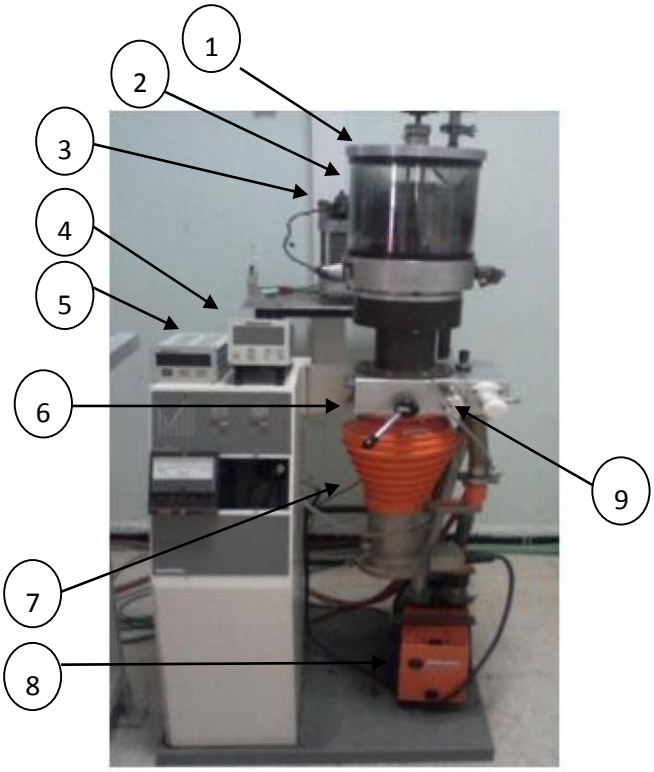

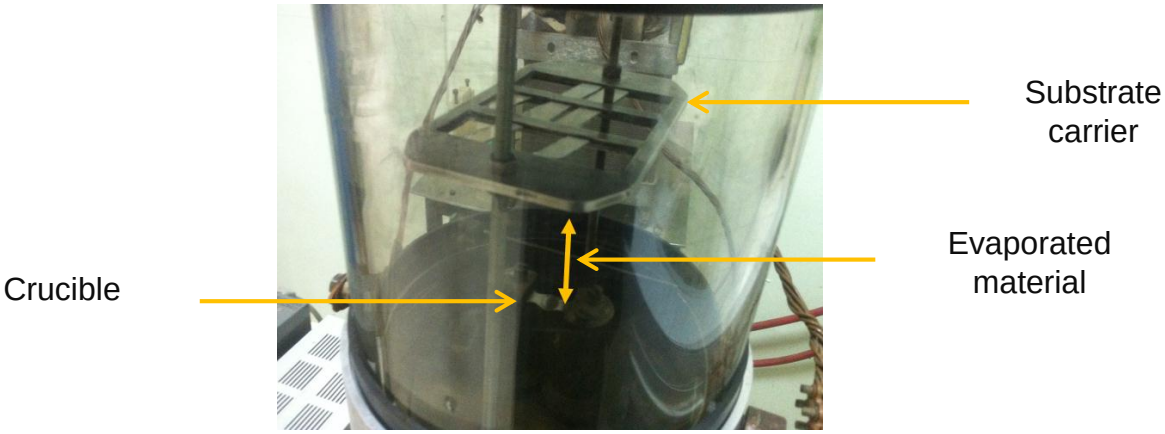

Fig.III-1: Photograph of the experimental vacuum thermal evaporation equipment (CDTA).

(1) The flange.

(2) Pyrex glass enclosure.

(3) The transformer.

(4) The secondary vacuum display box.

(5) The primary vacuum display box.

(6) The baffle: contains the control valves of the pumping system.

(7) The oil diffusion pump.

(8) The vane pump.

(9) The secondary gauge.

Before starting each experiment, we wait until a sufficient vacuum is reached within the chamber. First, we start the primary pumping until we reach a pressure of about 1.10^{-2} mbar, then we start the secondary pumping until around 10^{-6} mbar. After the vacuuming of the enclosure, the material will be evaporated using a crucible electrically heated by joule effect and finally the steam will condense on the substrates. The main parameters used to develop vanadium oxide layers are summarized in **Table.III-1**.

Tab.III-1: The main deposition parameters of VO_x films.

Parameters / Layers	Primary pressure (mbar)	Secondary pressure (mbar)	Work pressure (mbar)	Deposit time (s)
VO_x	$2.7x10^{-2}$	$4x10^{-5}$	$1.4x10^{-4}$	20

III.3 Layer development procedures

During our experiments, we used a vanadium pentoxide powder with a purity of 99.6%.

III.3.1 Choice of deposition substrate

The choice of substrate type is mainly related to the economic reasons, and their transparency, which is well suited for the optical characterization of films in the visible.

ii. Glass slide

We chose the glass slide because of its natural properties; it is an amorphous, insulating, transparent, chemically inert solid materialand is also a candidate for bolometer applications [79]. Samples that have glass as a substrate were used to determine structural, morphological, optical, electrical and mechanical properties. The glasses used during our work are object holder slats of type (Stairway), 1mm thick and 25x75 mm^2 of surface.

III.3.2 Preparation of substrates

The quality of the deposit and consequently that of the sample depends on the cleanliness and condition of the substrate. Cleaning is therefore a very important step; all traces of grease and dust must be removed. These conditions are essential for the proper adhesion of the deposit on the substrate, and for its uniformity (constant thickness). The process of cleaning the surface of substrates is as follows:

- The substrates are cut with a diamond tip pen.
- Degreasing in an acetone bath for 10 minutes.
- Washing in ethanol at room temperature in an Ultrasonic bath to remove traces of grease and impurities attached to the surface of the substrate for 10 minutes.
- Then cleaning with ionized water with Ultrasound for 5minutes.
- Drying with compressed air.

III.3.3. Annealing procedure

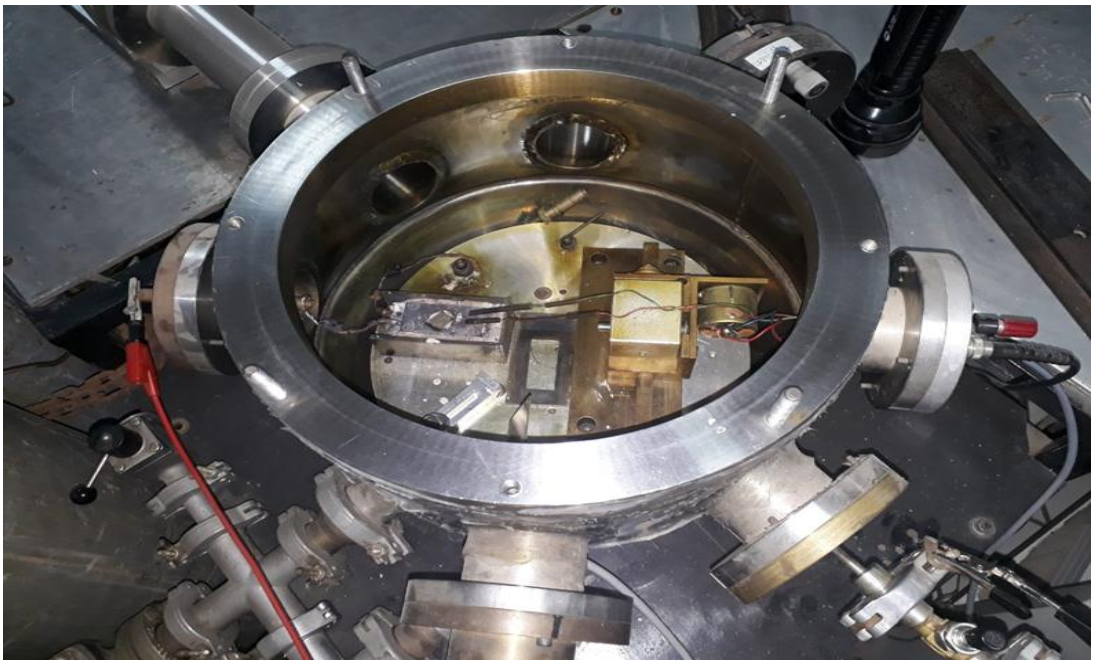

Fig.III-2: Photograph of the annealing device (CDTA).

After deposition, the samples underwent an annealing heat treatment in an oven under atmosphere at four different temperatures 400°C, 450°C, 500°C, 550°C.The temperature is measured by a REG48 **Thermo Regulator** witch is an instrument for controlling temperature. The temperature regulator takes an input from a temperature sensor, and has an output that is connected to a control element, such as a heater. To control the process temperature accurately, without significant intervention by the operator, the temperature control system relies on a real-time regulator that accepts a temperature sensor as input such as a thermocouple. It compares the actual temperature to the desired control temperature, or setpoint, and provides an output to a control element. The temperature regulator is part of the complete control system, and

the entire system must be analysed when selecting the corresponding temperature regulator.

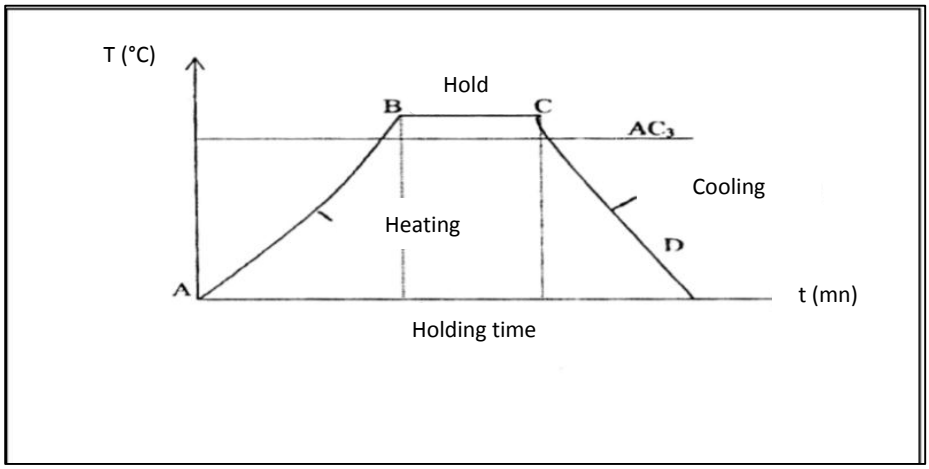

Fig.III-3: Characteristic of the heat treatment process.

The heat treatment process consists of:

- AB: Heating at temperatures above process temperature
- BC: Hold at a defined temperature
- CD: Cooling with a given rate

The annealing temperature was set at a range of 400°C-550°C with varying the holding time up to 90mn. The heating rate was fixed to 10°C/mn.

III.4 Characterization techniques for deposited films

In this section, the techniques used to study our layers are presented. Most of the characterizations were available at the CDTA advanced technology development centre laboratory level, which allowed us to perform a large part of the measurements on site. We have characterized vanadium oxide thin films by various methods: X-ray diffraction (XRD) and Raman spectroscopy for structural study, scanning electron microscopy (SEM) for microstructure and thickness study, and finally the electrical parameters such us sheet resistance, TCR, and noise to verify the quality of our films.

III.4.1. Structural and surface analysis

a. X-ray diffraction (DRX)

X-ray diffraction is a non-destructive analysis method and allows the determination of materials and mainly those with crystalline structure. The principle consists in irradiating the material to be analyzed with a monochromatic X-ray beam produced by an anticathode (copper or cobalt) and measuring the diffracted intensity according to the orientation of the coating grains. When Bragg conditions are met, diffracted X-rays constructively interfere. A diffraction peak proportional to the intensity of the reflected beam is observed (which shows in the figure.III-4. These diffraction peaks appear when the interplanar distance d and the incidence angle θ verify the Bragg law:

$$2d \sin\theta = n\lambda$$

With: θ is the angle of incidence of X-rays, n is the order of diffraction and λ is the wavelength of X-rays. This phenomenon was discovered by Max Von Laue (Nobel Prize winner in 1914) and studied at length by Sir William Henry Bragg and his son Sir William Lawrence Bragg (joint Nobel Prize winner in 1915).

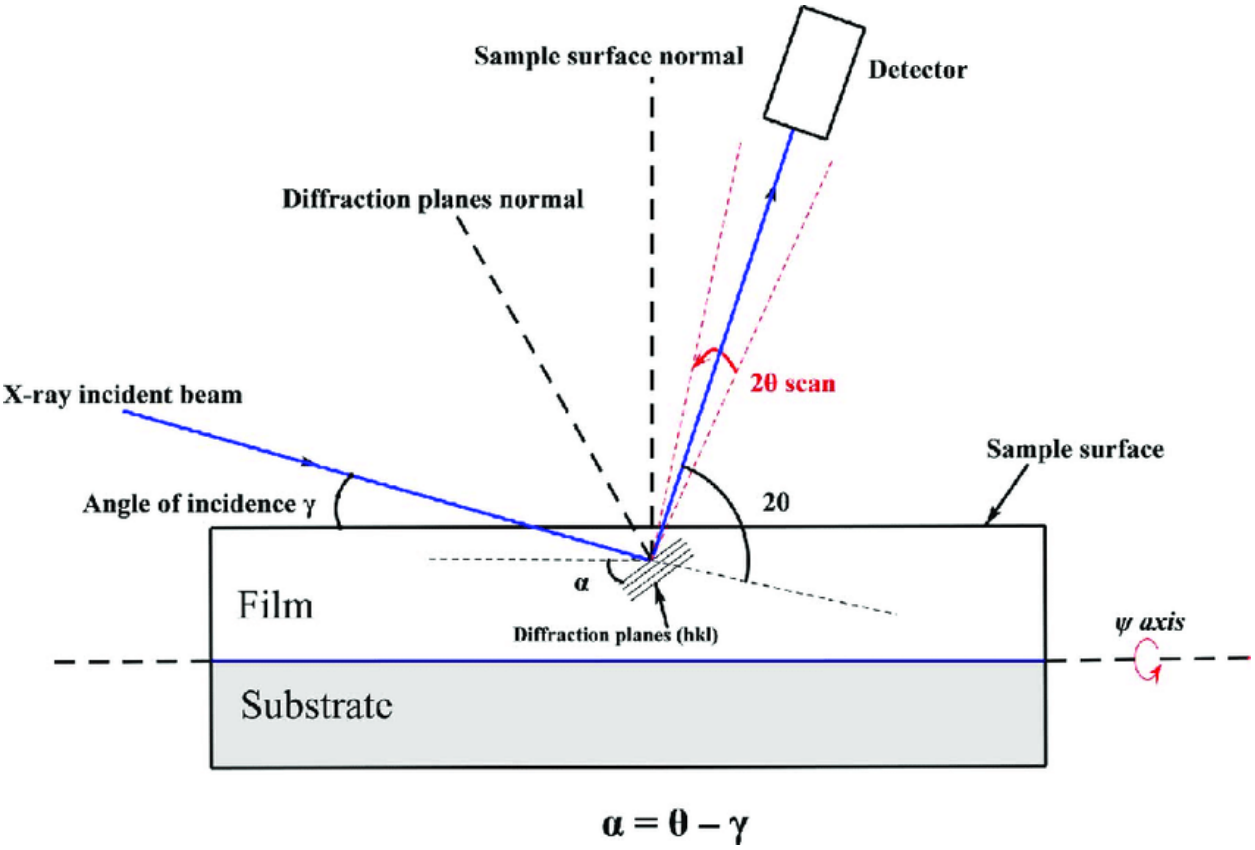

Fig.III-4: Schematic diagram of grazing incidence X-ray diffractometer [69].

The DRX characterization allowed us to:

- Identify the phases (position of the peaks)
- As well as the orientations of the films
- Stacking defects (peak shape)

The size of crystallites (diffracting domains) can be calculated from the diffraction diagrams on the surface of a sample using Debye Scherrer's law:

$$D = \frac{0.9\lambda}{w \cos\theta}$$

With: "D" the size of the crystallites, "λ" the wavelength of the X-ray beam, "W" the width at mid-height of the diffraction line and "θ" the diffraction angle.

In our experiment with X-ray diffraction measurements, we used a grazing configuration "$\alpha/2\theta$", the irradiated depth decreases proportionally with the angle of incidence of the X-ray beam. This decrease is related to the geometry of the assembly on the one hand and to the total reflection effect of the radiation on the other.

The incidence angle (angle between the incident beam and the surface) is fixed and of low value, by variation of the detector angle 2θ (only element rotating during the analysis), the entire spectrum is collected that shown in the figure above [81]. All measurements were made using a Bruker D8 ADVANCE diffractometer (CDTA). The source used is a copper cathode ($\lambda_{cu\text{-}k\alpha}$ = 1.54 Å).Diffraction patterns are collected at ambient temperature over an angular range of 10-88°.

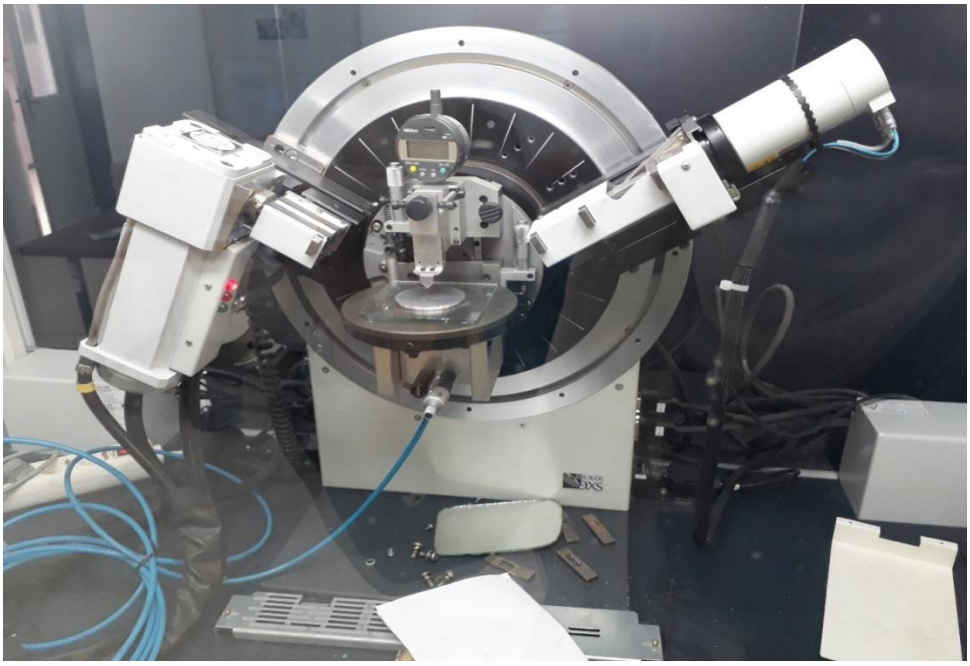

Fig.III-5: Photograph of the X-ray diffractometer Bruker D8 ADVANCE (CDTA).

b. Scanning Electron Microscope (SEM)

Scanning electron microscopy is a material imaging technique based on the principle of electron-matter interaction, capable of producing high-resolution images of

the surface of materials. The principle consists of an electron beam scanning the surface to be analysed which in response re-emits certain particles such as secondary electrons, Auger electrons, X-photons and light photons. These particles are analysed by different detectors that allow to reconstruct an image of the surface. The figure above illustrates the schematic diagram of how the SEM works.

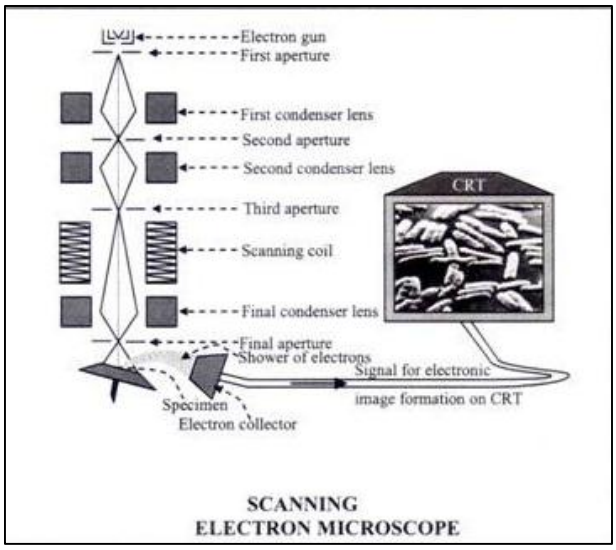

Fig.III-6: Ray diagram of a scanning electron microscope [82].

In our study, we used scanning electron microscopy (SEM) to identify the morphology of our films as well as the thickness estimation using samples made on glass substrates. The microscope used is a Jeol JSM-6360LV device with an acceleration voltage between 5kV-15kV (**Figure.III-7**).

Fig.III-7: Photograph of the scanning electron microscope (SEM).

III.4.2. Morphology and thickness analysis

- **Raman spectroscopy**

Raman spectroscopy is a non-destructive material characterization technique; its principle is based on the observation of molecular composition by exploiting the physical phenomenon of the modification of the frequency of light passing through any medium. This frequency offset is called the Raman Effect and corresponds to an energy exchange between the light beam and the medium, which provides information about the material. It consists of sending monochromatic light onto the sample and analysing the scattered light.

Raman spectroscopy corresponds to the inelastic scattering of light by molecules. The light scattered by the molecules contains Rayleigh photons, the majority of which have energy of $h\upsilon$ ($\upsilon = 1/\lambda$) equal to that of excitation $h\upsilon_{diff} = h\upsilon_0$, but also Raman photons, much less numerous, whose energy is modified by molecular vibration transitions: $h\upsilon_0 - h\upsilon_{vib}$ (Raman Stokes photons) and $h\upsilon_0 + h\upsilon_{vib}$

(anti-Stokes Raman photons). Being of higher probability (intensity), the Raman Stokes component is used by default in analytics.

Raman analyses were carried out in the CDTA characterization laboratory; measurements were made using a Raman spectrometer LabRam H-Revolution by Horiba JobinYvon (See figure below).

The monochromatic light source comes from a He-Ne gas laser, in our case we worked under these acquisition parameters as follows

Spectrum: 633nm-17mW (5%)-600gr/mm-x100vis-hole300-20s-3accs.

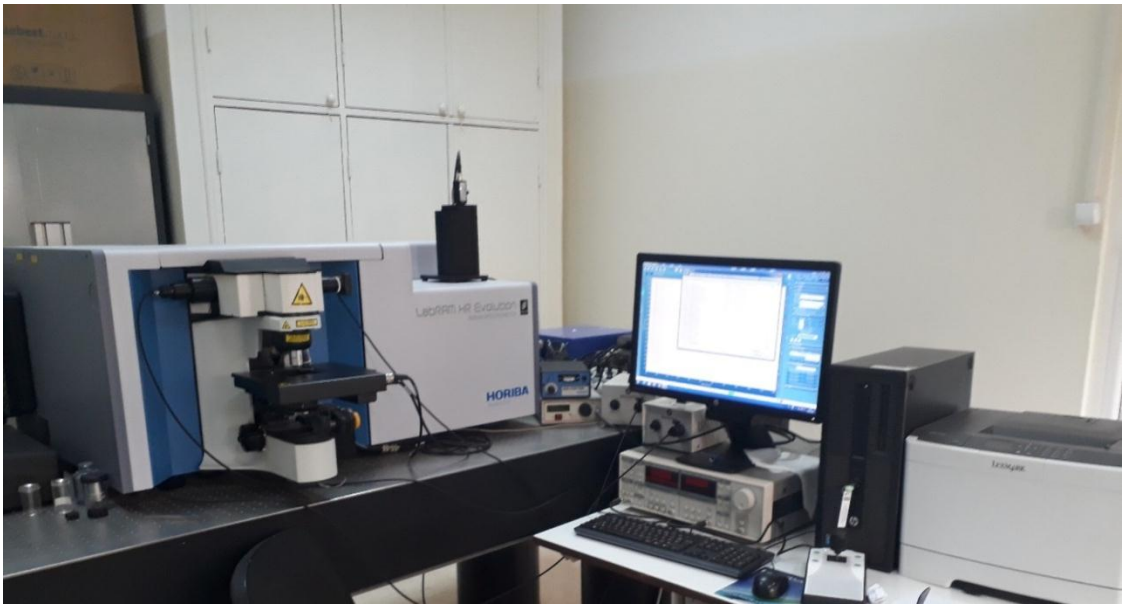

Fig.III-8 : Raman spectrometer device (CDTA).

III.4.3. Electrical properties analysis

- **Four-point technique**

Basic working principle of a four-point probe is measuring sheet resistance of a thin

Film on an insulating substrate. If the surface does not an insulator the sheet resistance cannot be measured.

In this study, sheet resistances of thin films were measured by four point probe. There are two probes which are connected a current supply are placed outer side of all dour point probes. The other two probes measure the voltage between two probes.

When the current applied, the voltage change is read from the inner probes. The relationship between current and voltage is dependent to the resistivity of the thin films.

A four-pointed mounting is available in the (CDTA) laboratory, the electrical measurement we have made are mainly current-voltage characteristic (I (V)), by varying the current from (0.1-10 µA) and measuring the voltage flowing in the sample.

These curves will be used to calculate resistance of the films from the slope of the linear curve I (V).

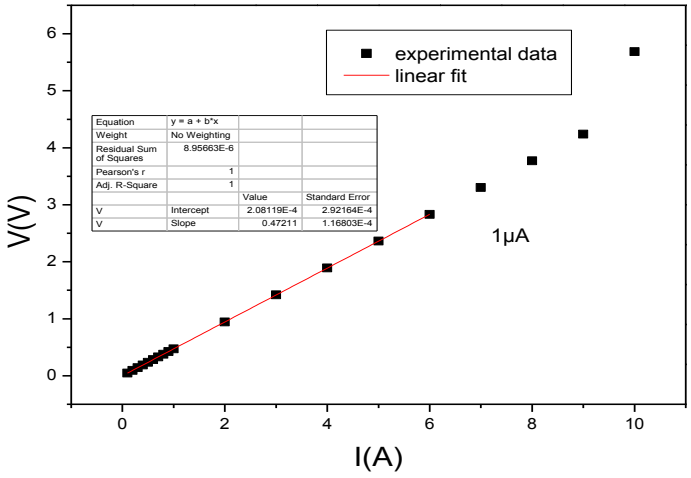

Fig.III-9: Current voltage characteristic.

After that the resistance of the films were measured, the samples were heated from ambient temperature to 90°C. The temperature is controlled by a REG48 thermo-regulator to reach 90°C at 30mn and the current was kept at 1µA.

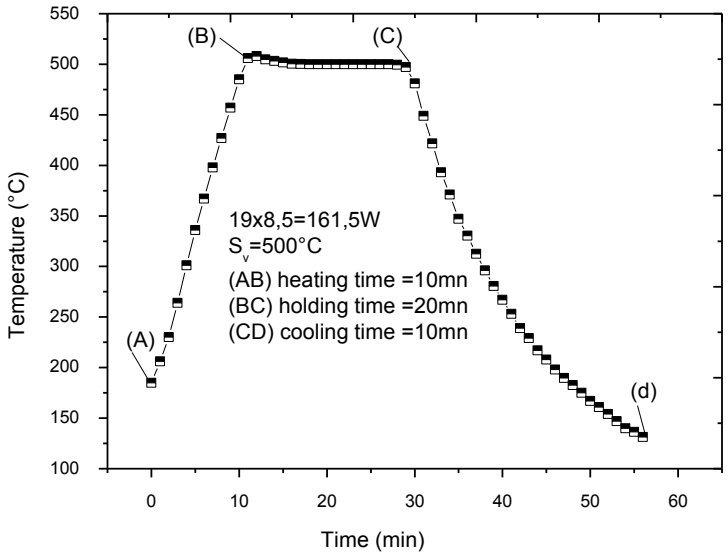

Fig.III-10: Heating process treatment.

The equipment is from Keithley's 2400C brand (200V, 1A, 20W Source Meter SMU Instrument with contact check). (See **Figure.III-11**).

Fig.III-11: Photograph of the four-pointed device (CDTA).

- **Experimental description of noise measurement**

After a polarization of the sample, the current is amplified and converted into voltage by an amplifier (transampedance). The output of this amplifier is connected to the sound card input (microphone input). An application developed under Labview allowed the acquisition and display of the current after a Fourier transformation (FFT). The figure shows a simplified diagram of the noise current measurement experiment.

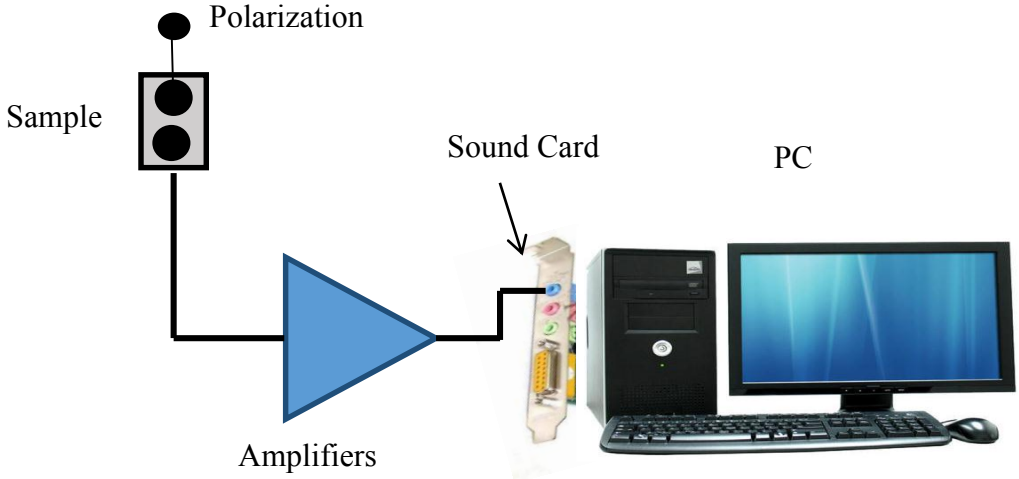

Fig.III-12: Schematic representation of the experimental of noise.

CHAPTER IV

Results and discussions

IV.1 Introduction

This chapter concerns the study of the experimental results of deposited vanadium oxide layers by thermal evaporation on substrates of glass; we will discuss the experimental results of the influence of the annealing temperature on the structural, morphological and electrical properties of the elaborate layers.

- For the structural study, we used the XRD and RAMAN.
- For the study of morphology, we used the electron microscope to scanning (SEM).
- The electrical properties have been studied to measure the resistance by the method of the four points at different temperatures.

Note that the present investigation thin films were prepared on ordinary glace substrates keeping all the deposition parameters fixed; we have only changed the time and the temperature of annealing.

IV.2 Structural characterizations

- **Series 400°C**

The x-ray diffraction patterns of the vanadium oxide thin films deposited by thermal evaporation and annealed at 400°C for different time (5min; 10min; 15min; 20min; 25mn; 30mn; 60mn; 90mn) revealed the absence of any prominent peaks, which confirm their amorphous like nature [87].

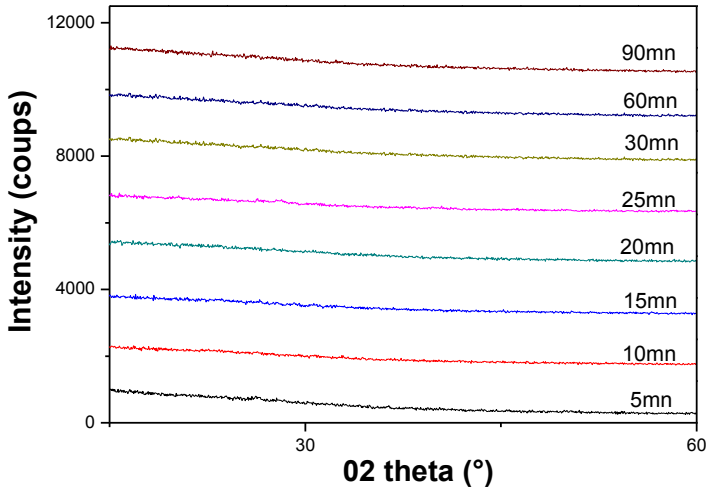

Fig.IV-1: XRD patterns of thermally deposited thin films annealed at 400°C for different time (5; 10; 15; 20; 25; 30; 60; 90) min.

- **Series 450°C**

The XRD patterns of **figure.IV-2** show that the as-deposited amorphous vanadium oxide thin films crystallise after post-annealing treatment. It can be observed that the crystallization starts at 450°C, showing the multi-oxide phase structure [84]. The XRD pattern for the simple which was annealed for 2.30min showed a height intensity in the (011) plan at 2θ=26.54° which correspond to V_4O_9 [86] phase and another less intense peak at θ=28.01° which is related to VO_2 (M1) (011) JCPD card [00-033-1441] [85]. With increasing the time of annealing at the same temperature to 5min, 10min and 15 min, we observed that the two peaks still in competition with VO_2 phase dominance for annealing time higher than 10min.

The samples annealed at 450°C for 20min, 25min and 30min showed additional reflection that correspond to another α-V_2O_5 growth direction (001) at 20.17° JCPD card [00-041-1426] [87] with the last two peaks at 26.54°(V_4O_9)(011) and 28.01°(VO_2)(011).

At 45min of thermal treatment GXRD pattern showed the absence of any diffraction peaks. However, a complete transformation into V_2O_5 pure phase was observed by Raman spectra in (**figure IV-3**) below [82].

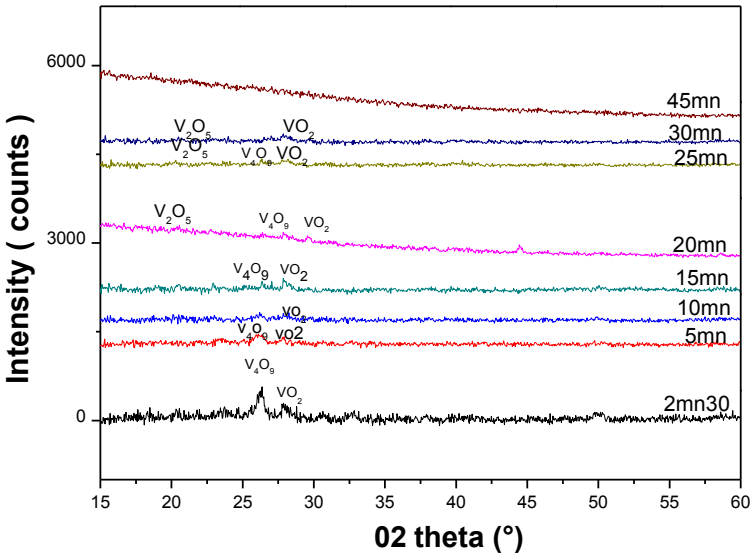

Fig.IV-2: XRD patterns of thermally deposited thin films annealed at 450°C for different time (2.30; 5; 10; 15, 20; 25; 30; 45) min.

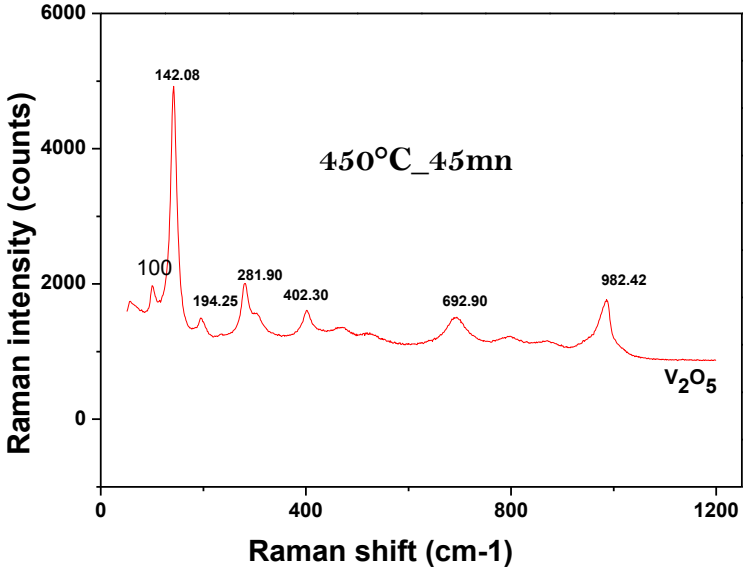

Fig.IV-3: Raman spectra of thermal evaporated and annealed vanadium oxide at 450°C for 45min.*

- **Series 500°C**

Figure.IV-3 shows x-ray diffraction pattern of the films annealed at 500°C for deferent time. The samples annealed for 5, 10 and 15 min shows a dominant phase which is VO_2 (M) (011) at 28.05° [84] and another peak at 26.50°which correspond to V_4O_9 (011) [85], after increasing the time to 20 and 25 min the last two phases still in competition and an additional reflection that correspond to V_2O_5 at 20.15° [86] has appeared.

At 30min of annealing we observe additional reflections corresponding to other growth of V_2O_5 with peaks (001) at 20.33°, (401) at 37.97°, (611) at 58.38° and (103) at 64.04° with less intense peaks of VO_2 and V_4O_9, with increasing the time to 45and 60min it's shown that the two phases VO_2, V_4O_9 disappears and we get only pure phase of V_2O_5 [87].

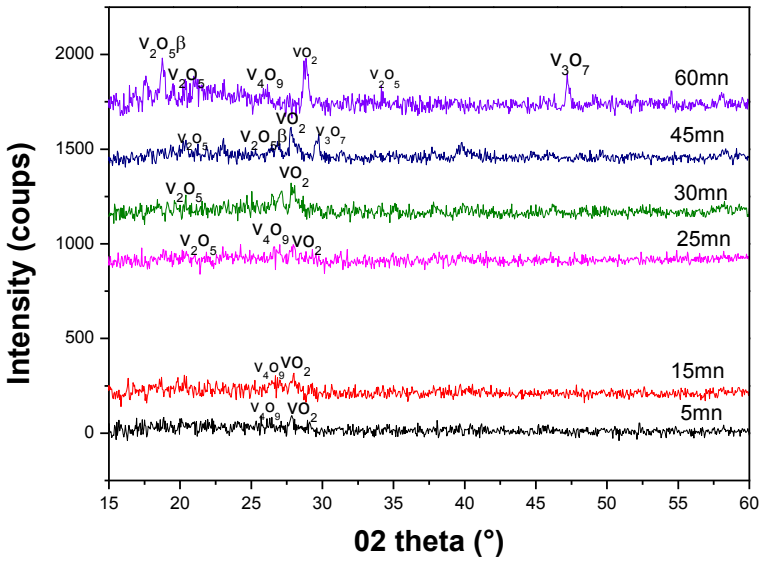

Fig.IV-4: XRD patterns of thermally deposited thin films annealed at 500°C for different time (5; 10; 15, 20; 25; 30; 45; 60) min.

IV.3 Surface morphology

Surface microstructures obtained through SEM analysis (top view) are depicted in **figure.IV-5** and show the effect of time and temperature of annealing on the samples surface.

The surface morphology image show that the surface of the sample annealed at 400°C is homogenous smooth and uniform (see **figure.IV-5**).The thickness of the films was determined from the cross-sectional SEM image and its 150nm. At 450°C ,the films have an irregular crystallized with different grain sizes and shape due to the presence of multi-phase in the same film (VO_2(011),V_4O_9(011)); the estimated crystallite grain size of annealed films at 450°C is around [10-27] nm which has been calculated using a Scherer's formula. When the simples were annealed at 450°C for 45min we observed grains on the shape of rectangle distant in different direction and disposed in stacked layers that's confirm our results by the structural characterisation XRD,RAMAN , further increasing the annealing temperature to 500°C led to the enlargement of crystallites as evidence in **figure.IV-6(b).**The size of the grains is around (28_31) nm, and the grains grow this in different directions because of the multiphase existence (VO_2, V_4O_9, V_2O_5).

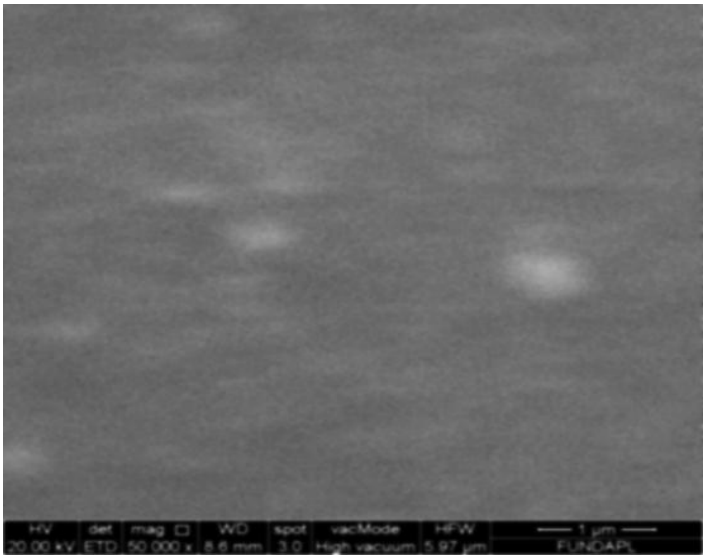

Fig.IV-5: SEM image of thermal evaporated and annealed vanadium oxide at 400°C for 30min.

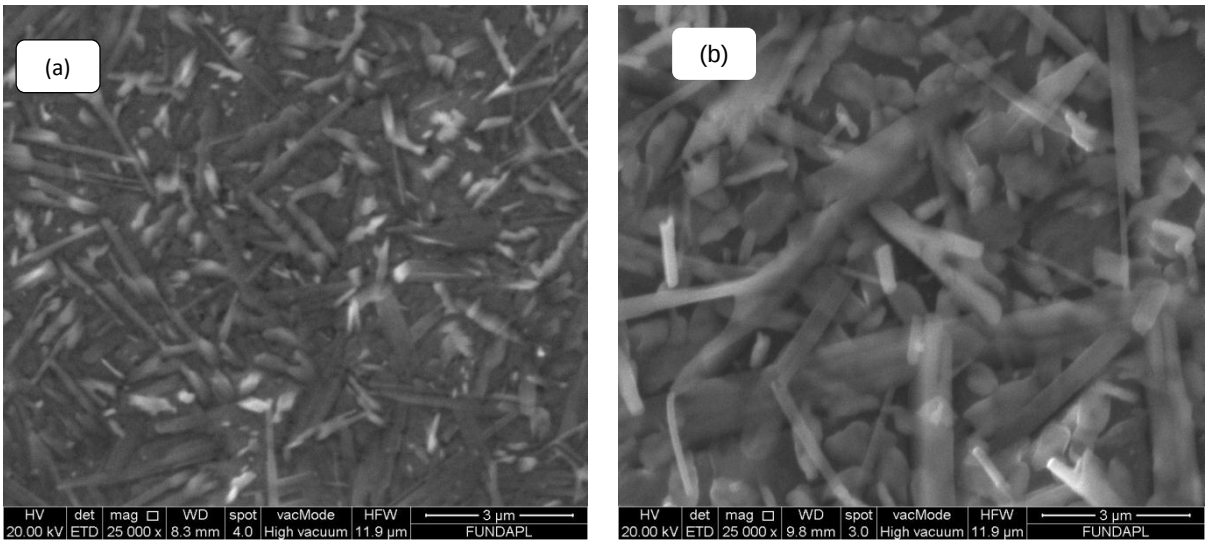

Fig.IV-6: SEM images of thermal evaporated and annealed vanadium oxide (a) at 450°C for 45min and (b) at 500°C for 45min.

IV.4 Electrical characterization

Thermal evaporated and annealed vanadium oxide thin films of thickness approximately 150nm were electrically characterized using 4points probe method under electrical current of 1µA. In the same time, a temperature sweep is performed in the range from 20°C_90°C with step of 1°C.

- **Electrical properties:**

The variation of electrical resistance with temperature for the samples annealed at deferent temperature is shown in figures below. A significant reduction in the resistance with the increase in the substrates temperature is observed and the variation is non-linear.

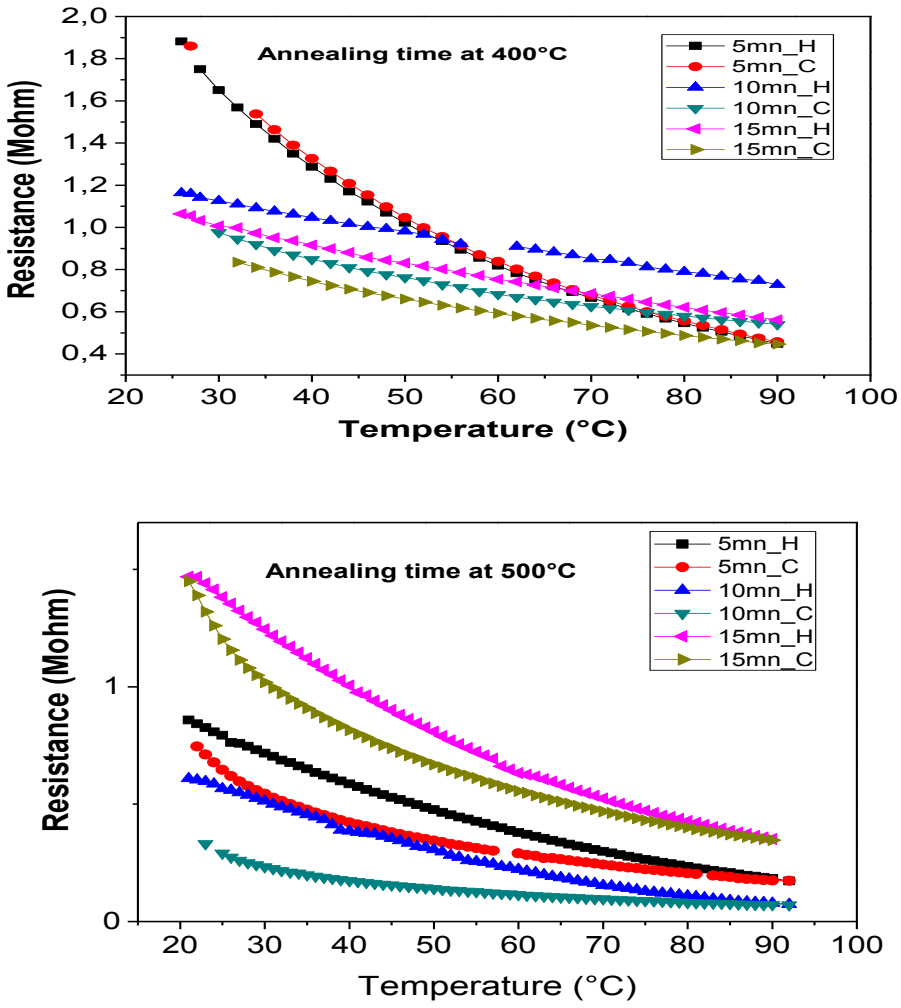

Fig.IV-7: Characteristics of VOx resistance vs. temperature of VOx films annealed at 400°C and 500°C.

No phase transition has been observed between the measured temperature intervals of 20°C to 90°C for the samples annealed at 400°C that was expected because the samples are amorphous. Even the samples annealed at 500°C although the layers do contain VO_2 but it doesn't transit this is may due to the structural defect caused by the high temperature. (See **Figure.IV-7**)

We have measured only the samples annealed for 5, 10 and 15min because when the time of annealing was increased above 15min, gaps between adjacent grains

appear due to the agglomeration effect .as a result continues uncovering of substrate is producing [87].

The annealed samples at 450°C for 5min, 10min, 15min and 20min exhibits a resistance drops due to the appearance of VO_2 phase , curves with hysteresis contain phases that undergo Insulator–Metal Transition in the temperature range applied .it is well known that the Insulator-Metal Transition in vanadium oxide has a hysteresis cycle during the heating-cooling cycle. Oxide vanadium that undergoes this transition in the applied temperature range is the VO_2. (See **figure.IV-8**)

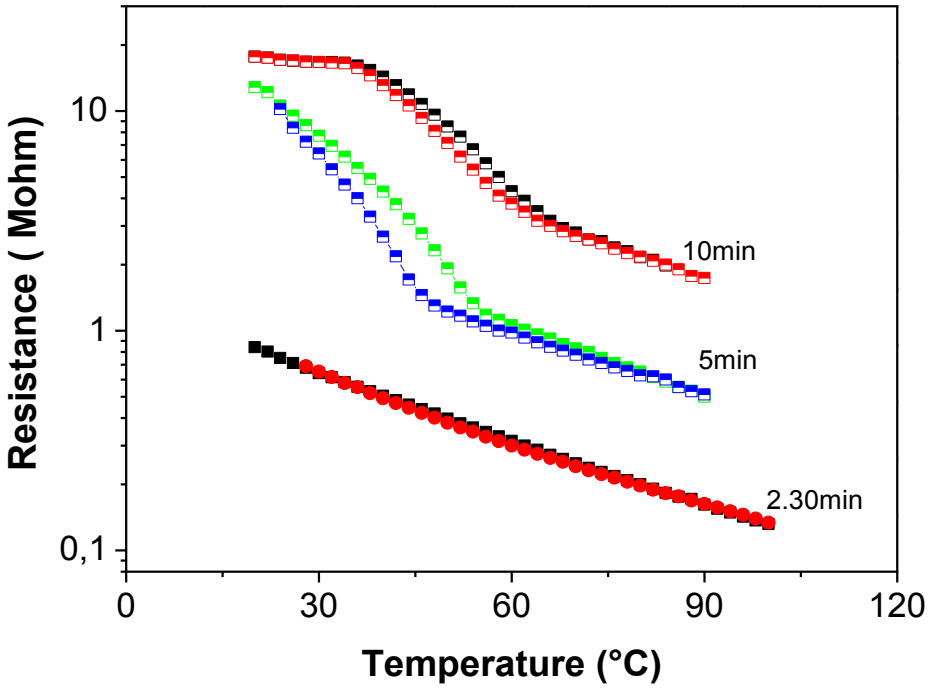

Figure.IV-8: Characteristics of the resistance vs. temperature of VOx films annealed at 450°C.

a. Temperature Coefficient of Resistance TCR

After resistance measurements, TCR and resistivity measurements were done between 20°C and 90°C for all the films and the results are shown in the table below. (All the TCR value are taken at room temperature 25°C).

TCR is the measure of how rapidly the electrical resistance of a material responds to the change in temperature [89] and it's defined as the change in resistance of the sensing material per degree change in temperature, TCR is expressed as

$$TCR = 1/R(dR/dT)$$

Where R is the resistance of the device and T is the temperature [88].

We clearly see from the table below that TCR value are high enough to use in a microbolometer applications for every temperature of annealing even with small time of annealing, a remarkable TCR values are obtained at the sample annealed at 450°C for 2min30 measuring 2.43%/°K with a resistivity 135.9 ohm.cm (the low resistivity is due to the presence of V_4O_9 phase in all the films ,as known V_4O_9 is metallic at room temperature and low hysteresis, the sample show a multi-oxide phase structure (V_4O_9, VO_2, V_2O_5) by XRD and the sample annealed at 400°C for 5min measuring 2.58%/°K with resistivity 127.75 Ohm.cm and low hysteresis, this result strongly agree with the literature [89,90,91,92].

It's remarkable that the resistivity of our films is high than the range of the resistivity cited in the literature ranging for (0.1_10) ohm.cm [93], but it's possible to solve the problem of high resistivity in vanadium oxide thin films for infrared imaging [93].

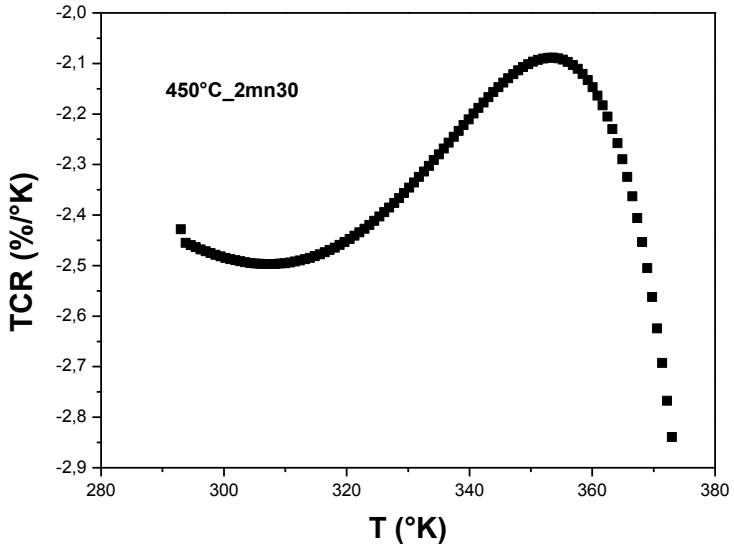

Fig.IV-9_a: TCR of the sample at 450°C for 2mn30.

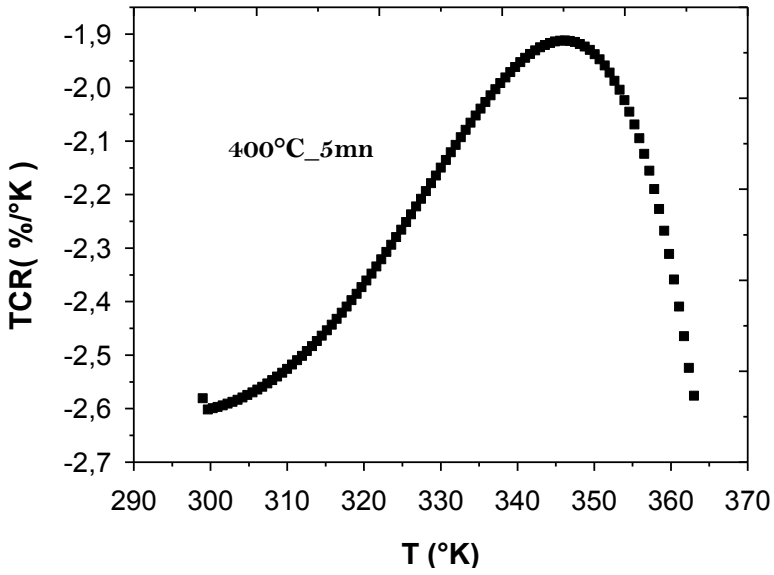

Fig.IV-9_b: TCR of the sample 400°C_5mn.

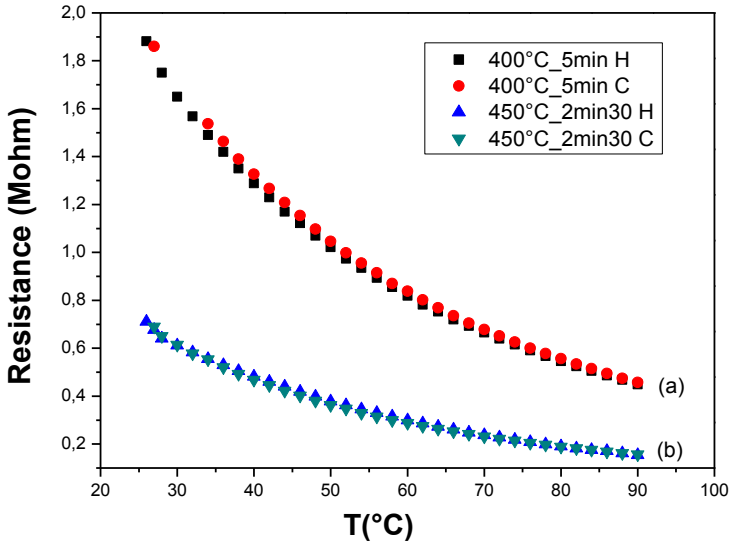

Fig.IV-10: shape of hysteresis of the samples (a) 400°C_5min and (b) 450°C_2min30.

During TCR calculations of the samples annealed at 450°C for 10min and 400°C for 90min, we noticed a high value of TCR (7%/°K) and (5%/°K) respectively at high temperatures. Figure bellow show high TCR at high temperature for the sample annealed at 450°C for 10min but this last contain VO_2 as principal phase and it shows an hysteresis effect which is unsuitable for microbolometer application, it is important for pratical use to minimize hysteresis of electrical resistance when VO_x thin films are used for bolometer application.

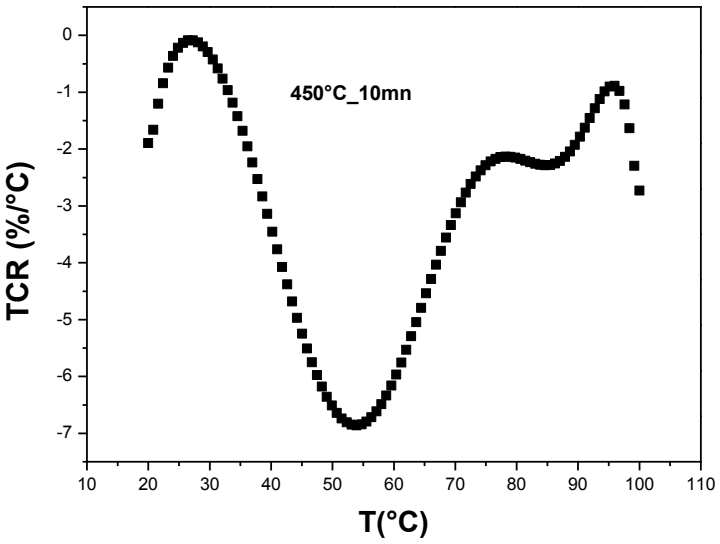

,

Fig.IV-11: TCR of the sample at 450°C for 10min.

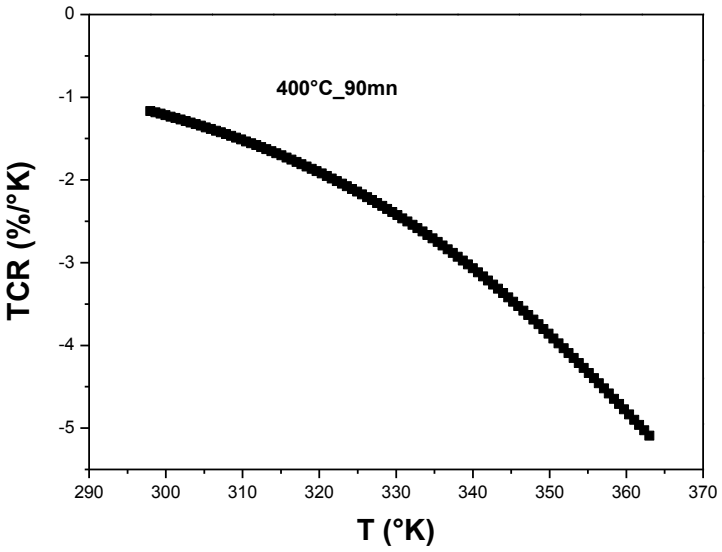

Fig.IV-12: TCR of the sample 400°C_90min.

Tab.IV-1: Resistivity and the TCR at different temperatures and annealing times.

Annealing temperature (°C)	Annealing time (mn)	TCR (%/°K)	Resistivity (ohm.cm)
400°C	5 10 15 30 60 90	2.58 1.29 1.83 1.92 1.72 1.17	135.9 78.82 67.95 45.57 54.36 27.18
450°C	2mn30 5 10 15 25 45	2.43 1.56 1.90 1.20 1.89 -1.43	127.75 873.2 1155.15 183.5 34 34
500°C	5 10 15	1.89 2.07 2	122.31 101.92 203.85

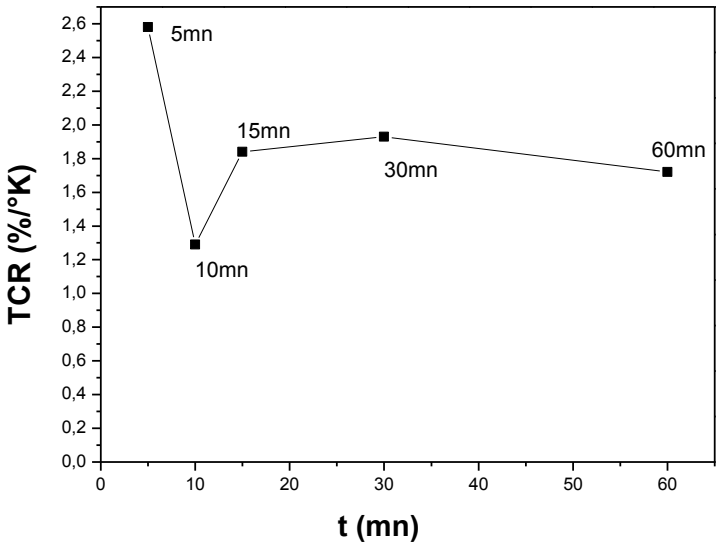

Fig.IV-13: TCR at room temperature for different annealing time for VOx films annealed at 400°C.

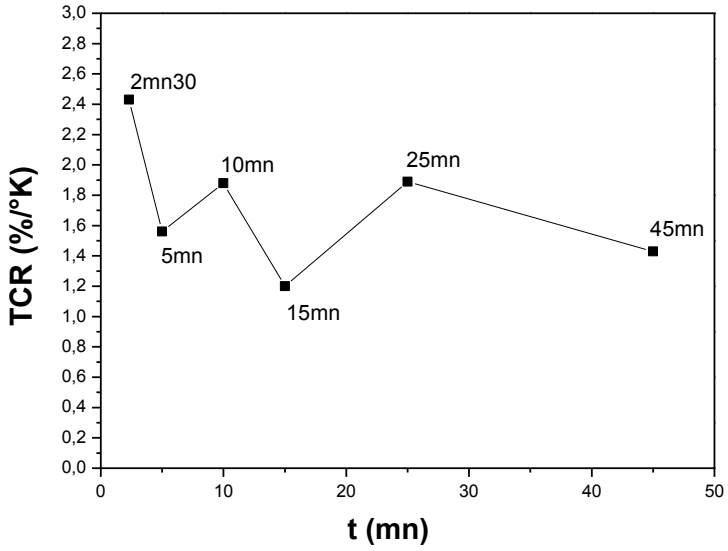

Fig.IV-14: TCR at room temperature for different annealing time for VOx films annealed at 450°C.

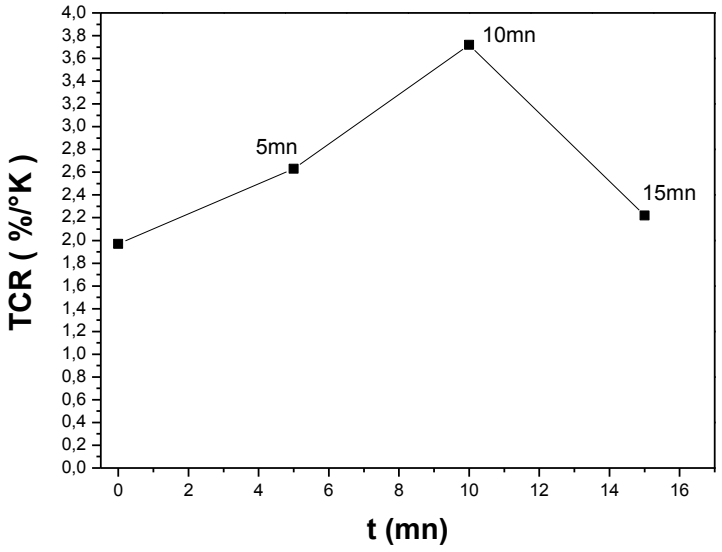

Fig.IV-15: TCR at room temperature for different annealing time for VO_x films annealed at 500°C.

The figures above shows that the high values of TCR were obtained at short time of annealing (400°C_5min with TCR=2.57%/°K; 450°C_2.30min with TCR=2.43%/°K). Those TCRs values are conjugated with relatively low resistivity and non-hysterises behavior.

b. Noise measurement

In semiconductor components, thermal agitation, interactions between free electrons and shocks between carriers and crystal lattice particles cause thermal noise. The studies have shown that this noise is independent of frequency, that it is white noise and that it depends only on the resistance of the component under study and its temperature. [94]

The spectral density of the thermal noise current is defined by the following equation:

$$S_I(f) = \frac{4KT}{R}(A^2|Hz)$$

T: Temperature of the device under test (°K)

K: Boltzmann constant equal to 1.3806488 x $10^{-23} m^2 K g S^{-2} K^{-1}$

R: Resistance of the component under test.

Noise measurement has been done for the sample (450°C_2.30min) which showed lower resistivity among samples and higher TCR and non-hysteresis.

Figure.IV-16 shows the measurements of power spectral density (PSD) for VO_x samples as a function of frequency for different bias voltage.

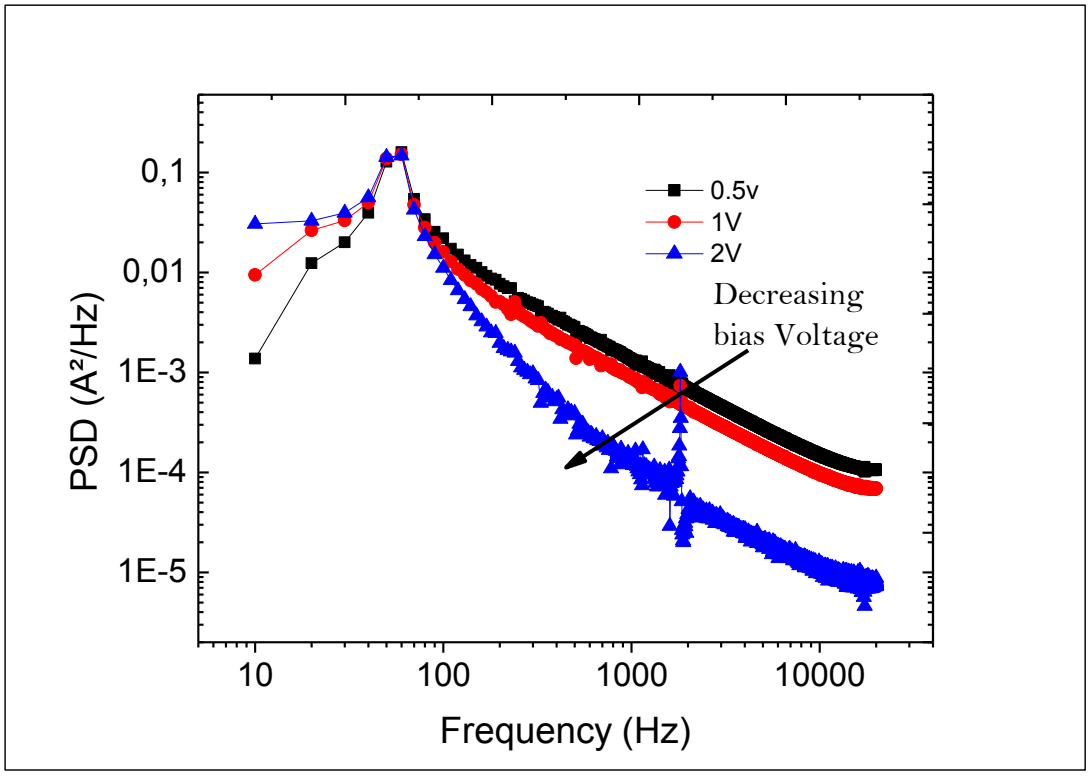

Fig.IV-16: Power Spectral Density (SI) as a function of frequency for different bias voltages of the sample (450°C_2.30min).

The noise measurements were carried out at bandwidth of 20000 Hz. The total noise voltage per unit bandwidth was found to decrease with increasing the bias voltage at room temperature. **(Figure.IV-16)**

IV.5 Conclusion

In this chapter, we have studied the influence of temperature on the properties of vanadium oxide films; we made several sets of samples that we have characterized structurally, morphologically and electrically. The effect of the annealing is very remarkable on the different properties of the layers filed. TCR and resistivity where measured for low temperature (from ambient to 90°C) we found that the values are coinciding with the reported TCR [2-3]%/°K values of successful vanadium oxide thin films deposited at by other techniques.

GENERAL CONCLUSION

The work presented in this thesis deals with the development and study of the properties of vanadium oxide thin films. To make these deposits, we used thermal evaporation from a V_2O_5 powder. This technique makes it possible to obtain deposits having properties depending on the development conditions. We then carried out heat treatments under air, to study their effects on composition and structure of thin layers made

We have characterized the thin layers of vanadium oxide by various methods: X-ray diffraction (XRD), Raman spectra for structural study, scanning electron microscopy (SEM) for the study of the microstructure, and finally the method of the four points to determine the electrical properties of our layers. We particularly focused our attention on the influence of heat treatments.

It has been found that the change of temperature and the annealing time play an important role in the crystallization and oxidation of the elaborated layers. Not only on the microstructure and crystalline orientation, but also on the phase composition of thin layers.

In the second part, our work focused on the characterization of these layers elaborated which allowed us to draw the following

From the results it can be concluded that, it is impossible to obtain pure phases of vanadium with low oxidation like VO_2 using thermal evaporation technique and annealing process.in the other hand it’s possible to get mixture of VOx in the same film.

The electrical measurements that we obtained by the technique of the four points, allows to draw that using thermal evaporation process following by specific annealing condition allow to have thin films of mixture of vanadium oxide with a moderate resistivity ranging from(27_135)ohm.cm for the films annealed at 400°C,(34_1155)ohm.cm for the films annealed at 450°C and (101_203)ohm.cm ,high TCR (2.58,2.43,2)%/°K and low noise at room temperature, which is promising for using the films in microblometer application.

After studying all the characterizations of our films we can conclude that the best vanadium oxide thin films for microbolometer application was obtained at small time of annealing (2.30mn_10mn).

Bibliographical references

[1]K.Schneider,M.Lubecka,A.Czapla,V_2O_5thinfilmsforgassensorapplications,Sens.Actuators,B236(2016)970–977.

[2]P.DeepakRaj,S.Gupta,M.Sridharan,NanostructuredV_2O_5thinfilmsdepositedatlowsputteringpower,Mater.Sci.Semicond.Process.39(2015) 426–432.

[3]Tuan Duc Vu, Zhang Chen, Xianting Zeng, Meng Jiang, Shiyu Liu, YanfengGao and Yi Long « Physical vapour deposition of vanadium dioxide for thermochromic smart window applications »

[4] D. VOLUER, article « Vanadium et Composés ».

[5] B. M. Vasyutinskiy, G. N. Kartmazov, Yu. M. Smirnov, and V. A. Finkel, *Phys. Met. Metall.*, 1966, **21**, 134. transition. J. Phys. Chem. Solids 31, 2569–2575 (1970).

[6] Zou C.W., Yan X.D., Han J., Chen R.Q. and Gao W., Microstructures and optical properties of β-V2O5 Nano rods prepared by magnetron sputtering. J.Phys D: App Phys. 2009; 42(14):145402. DOI: 10.1088/0022-3727/42/14/145402

[7] Jayaraman, A., McWhan, D. B., Remeika, J. P. & Dernier, P. D. Critical Behavior of the Mott Transition in Cr-Doped V2O3. Phys. Rev. B 2, 3751–3756 (1970).

[8] Kuwamoto, H. &Honig, J. M. Electrical properties and structure of Cr-doped nonstoichiometric V_2O_3. J. Solid State Chem. 32, 335–342 (1980).

[9] https://images.app.goo.gl/PGwdN1uGtcijuXVb8

[10]Dernier, P. D. &Marezio, M. Crystal Structure of the Low-Temperature Antiferromagnetic Phase of V_2O_3. Phys. Rev. B 2, 3771–3776 (1970).

[11]McWhan, D. B. et al. Electronic Specific Heat of Metallic Ti-Doped V2O3. Phys. Rev. Lett. 27, 941–943 (1971).

[12]Kokabi, H. R., Rapeaux, M., Aymami, J. A. &Desgardin, G. Electrical characterization of PTC thermistor based on chromium doped vanadium sesquioxide. Mater. Sci. Eng. B 38, 80–89 (1996).

[13] McWhan, D. B. &Remeika, J. P. Metal-Insulator Transition in $(V_{1-x}Cr_x)_2O_3$. Phys. Rev. B 2, 3734–3750 (1970).

[14] McWhan, D. B., Rice, T. M. &Remeika, J. P. Mott Transition in Cr-Doped V_2O_3. Phys. Rev. Lett. 23, 1384–1387 (1969).

[15] Menth, A. &Remeika, J. P. Magnetic Properties of $(V_{1-x}Cr_x)_2O_3$. Phys. Rev. B 2, 3756–3762 (1970).

[16] Moon, R. M. Antiferromagnetism in V_2O_3. Phys. Rev. Lett. 25, 527–529 (1970).

[17] Shivashankar, S. A. &Honig, J. M. Metal—antiferromagnetic-insulator transition in V2O3 alloys. Phys. Rev. B 28, 5695–5701 (1983).

[18] Brockman, J. electric field-induced conductivity switching in vanadium sesquioxide nanostructures. (Stanford University, 2012).

[19] Metcalf, P. A. et al. Electrical, structural, and optical properties of Cr-doped and non-stoichiometric V_2O_3 thin films. Thin Solid Films 515, 3421–3425 (2007).

[20] A. GIES, « Synthèse et caractérisation de couches minces de V2O5 dopé ou non pour une utilisation dans des microbatteries au lithium », thèse doctorat, université de BORDEAUX, 14 décembre 2005.

[21] V.V. Atuchin, B.M. Ayupov, V.A. Kochubey, L.D. Pokrovsky, C.V. Ramana ,Yu.M. Rumiantsev «Optical properties of textured V2O5/Si thin films deposited by reactive magnetron sputtering», Opt Mat 30 (2008) 1145–1148.

[22] Ch. TENAILLEAU, «synthèse et caractérisation de sesquioxydes de vanadium et molybdène à transition Métal/isolant», thèse doctorat, université Maine, année 2001.

[23] L.Q.Mai, B.Hu, W. Chen, and E.D.Gu, «Electrical property of Mo-doped VO2 nanowire Array Film by melting-Quenching sol-gel methode», 2006, 110, 19083-19086.

[24] Troy D. Manning, Ivan P. Parkin, Martyn E. Pemble, David Sheel, and DimitraVernardou, «Intelligent Window Coatings: Atmospheric Pressure

Chemical Vapor Deposition of Tungsten-Doped Vanadium Dioxide», Chem. Mater. 2004, 16, 744-749.

[25] Xiaochun Wu, Fachun Lai, Limei Lin, Yongzeng Li, Lianghui Lin, Yan Qu, Zhigao Huang, «Influence of thermal cycling on structural, optical and electrical properties of vanadium oxide thin films», App Surface Science 255 (2008) 2840–2844.

[26] B.V.L'vov, V. L. Ugolkov and F.F. Grekov, Thermochimicaacta 411(2004)187.

[27] Langmuir. Amer. Chem. Soc.37 (1915)1139.

[28] V. E. Henrich& P. A. Cox, the Surface Science of Metal Oxides. Cambridge University Press, 1994.

[29] S. P. Lim, J. D. Long, S. Xu, et K. Ostrikov, « Nanocrystalline Vanadium Oxide Films Synthesized by Plasma-Assisted Reactive RF Sputtering Deposition », J. Phys. D. Appl. Phys., vol. 40, no 4, p. 1085-1090, févr. 2007.

[30] S. Beke, « A Review of the Growth of V_2O_5 Films from 1885 to 2010 », Thin Solid Films, vol. 519, no 6, p. 1761-1771, janv. 2011.

[31] D. H. Hensler, « Transport Properties of Sputtered Vanadium Dioxide Thin Films », J. Appl. Phys., vol. 39, no 5, p. 2354, 1968.

[32] F. Rivera, L. Burk, R. Davis, et R. Vanfleet, « Electron Back-scattered Diffraction of Crystallized Vanadium Dioxide Thin Films on Amorphous Silicon Dioxide », Thin Solid Films, vol. 520, no 7, p. 2461-2466, janv. 2012.

[33]K. Sieradzki, K. Bailey, and T. L. Alford« Agglomeration and percolation conductivity»Applied Physics Letters 79, 3401 (2001); doi: 10.1063/1.1419043.

[34] S.Cho, J.Ma, Y.Kim, Y.Sun, K.L.GeorgreAppl.Phys.Lett 75(1999)2761

[35] https://images.app.goo.gl/w11n1xnW28sRwecW8

[36] https://images.app.goo.gl/Am4nFy5LnSt5EDDr8

[37] Zheng Wei Pan, ZuRong Dai, Zhong Lin Wang, Science291,(2001)1947.

[38] H.J. Yuan, S.S. Xie, D.F. Liu, X.Q. Yan, Z.P. Zhou, L.J. Ci, J.X. Wang, Y. Gao, L. Song, L.F. Liu, W.Y. Zhou, G. Wang.Chemical Physics Letters 371(2003)337-341.

[39] A.Moustaghfir, E. Tomassella, S.Ben Amor, M. Jacquet, J. Cellier, T. Sauvage, Surface and Coatings Technology 174-175 (2003) 193-196.

[40] Sarkar A, Gosh S, Chaudhuri S, Pal AK. Thin Solid Films (1991); 204:255.

[41] https://images.app.goo.gl/anDXqrM5USmhzaVP7

[42] C.Kitell. Introduction a la physique du solide Willey .New York (1966). [37] Major S, Banerjee A, Chopra K L. Thin Solid Films 1984; 122; 31.

[43] P. Nunes, E. Fortunato, R. Martins. International Journal of Inorganic Materials 3 (2001) 1125-1128.

[44] Tauc. J. Grigorovici R. and Vancu. Phys. Stat. Solid. (1996).9.627.

[45] P.Nunes, B.Fernandez, E. Fortunato, P. Vilarinho, R. Martins, Thin Solid Films 337 (1999) 76.

[46] H-Y. Bae, G-M.Choi, Sens. Actuators, B.Chem. 55 (1999)47.

[47] B.J.Lonkhande, P.s.Patil, M.D.Uplane; Materials letters 57(2002)573-579.

[48] C.H.Lee, L.Y. Lin, Appl. Surf. Sci. 92 (1996) 163.

[49] F.K Shan, Y. S. Yu. Journal of the European Ceramic Society. Vol 24, Issue6 (2004), 1869-1872.

[50] H. Demiryont, K.E. Nieternig, Solar Energy Materials, 19 (1989) 79.

[51] C.C.F. John, J.B. Frank, J. Electrochem. Soc.: Solid-State. Sci. Technol, 122(1975) 1719.

[52] B. Mebarki, Thèse Université de Toulouse, 1997.

[53] V. Srikant et D. R. Clarke, J. App. Phys., 81 (1997) 6357.

[54] https://images.app.goo.gl/hfq85vMtMKYczo988

[55] I.V. Kityk, J. Ebothe, A. Elhichou, M. Addou, A. Bougrine and B. Sahraoui, J. Phys. Condens Matter (14), pp.5407-5417 (2002).

[56]: B.J. Jin, S.H. Bae, S.Y. Lee, S. Im. Mat. Sci& Eng., B71 (2000) 301.

[57] S. Faÿ, thèse de doctorat, Institut de production et robotique, école polytechnique fédérale de LAUSANNE, N° 2899 (2003), France.

[58] Handbook of Chemistry and Physics, 56th Edition, 1975, Ed. R.C. Weast, CRS Press.

[59] https://images.app.goo.gl/YAyfE9p1x9ZC4waJ6

[60] W.S. Hu, Z.G. Liu, S.N. Zhu, Q.Q. Xu and D. Feng, Z.M. Ji, J. Phys. Chem. Solids, 58 (1997) 953.

[61] S.S. Kim, B.-T. Lee, Thin Solid Films, 446 (2004) 307.

[62] K. Matsubara, P. Fons, K. Iwata, A. Yamada, K. Sakurai, H. Tampo, S. Niki, Thin Solid Films, 431-432 (2003) 369.

[63] Sengodan, R., Shekar, B. C., & Sathish, S. (2013). *Morphology, Structural and Dielectric Properties of Vacuum Evaporated V2O5 Thin Films. Physics Procedia, 49, 158–165.* doi:10.1016/j.phpro.2013.10.022.

[64] S.-J. Jiang, C.-B. Ye, M. S. R. Khan, and Claes-Goran Granqvist “Evolution of thermochromism during oxidation of evaporated vanadium films”, Vol. 30, No. 7 / App Opt

[65] R. Santos, J. Loureiro, A. Nogueira, E. Elangovan, J.V. Pinto,J.P. Veiga, T. Busani, E. Fortunato, R. Martins, I. Ferreira, Thermoelectric properties of V2O5 thin films deposited by thermal evaporation, Applied Surface Science(2013),http://dx.doi.org/10.1016/j.apsusc.2013.06.016.

[66] Ashvani Kumar, Preetam Singh, Nilesh Kulkarni, Davinder Kaur “Structural and optical studies of nanocrystalline V2O5thin films” 2007 Elsevier B.V. All rights reserved.doi:10.1016/j.tsf.2007.04.165.

[67] Luís Henrique Cardozo Amorina, Alexandre Urbanoa “Commitment Between Roughness and Crystallite Size in the Vanadium Oxide Thin Film opto-electrochemical Properties”, DOI: http://dx.doi.org/10.1590/1980-5373-MR-2018-0245.

[68] S.-J. Jiang, C.-B. Ye, M. S. R. Khan, and Claes-Goran Granqvist “Evolution of thermochromism during oxidation of evaporated vanadium films” Vol. 30, No. 7 / App opt.

[69] P.Duval. High vacuum production in the microelectronics industry, Elsivier Ed, Amsterdam, (1988).

[70] Cours sur les couches (post-graduation) département physique.

[71] Langmuir. Amer. Chem. Soc.37 (1915)1139.

[72] Noua BOUHSSIRA. Élaboration et Caractérisation des Couches Minces d’Oxyde de Zinc par Evaporation. UNIVERSITE MENTOURI – CONSTANTINE.2015.

[73] R T Rajendra kumar1, BKarunagaran, D Mangalaraj , Sa K Narayandass,

P Manoravi, M Joseph and Vishnu Gopal. Study of a pulsed laser deposited vanadium oxide based microbolometer array.2003.

[74] https://images.app.goo.gl/o5tZ9K2EUzshhZfFA

[75] JCPD Card [01-071-2248].

[76] https://images.app.goo.gl/TzTzLerwk1zMFHLy6

[77] Ali, A.M., Abdel Hakeem, A.M., 2010. Phy.Status solid A207, 1, 132-138.

[78] Hongchen Wang ,Xinjian Yi , Sihai Chen. Infrared Physics & Technology 47 (2006) 273–277.

[79] JCPD Card [071-0565]

[80] JCPD Card [00-041-1426]

[81] Su, Y.-Y., Cheng, X.-W., Li, J.-B., Dou, Y.-K., Rehman, F., Su, D.-Z., & Jin, H.-B. (2015). Evolution of microstructure in vanadium oxide bolometer film during annealing process. Applied Surface Science, 357, 887–891. doi:10.1016/j.apsusc.2015.09.068

[82] A Subrahmanyam, Y Bharat Kumar Reddy and C L Nagendra “Nano-vanadium oxide thin films in mixed phase for microbolometer applications” J. Phys. D: Appl. Phys. 41 (2008) 195108 (6pp) doi:10.1088/0022-3727/41/19/195108.

[83] Zhou, C., Mai, L., Liu, Y., Qi, Y., Dai, Y., & Chen, W. (2007). Synthesis and Field Emission Property of V2O5·nH2O Nanotube Arrays. The Journal of Physical Chemistry C, 111(23), 8202–8205. doi:10.1021/jp0722509.

[84] A. Rogalski “Recent progress in infrared detector technologies”, Infrared Physics & Technology 54 (2011) 136–154.

[85] JCPD Card [033-1441]

[86] JCPD Card [031-1438]

[87] JCPD Card [034-0187]

[88] JCPD Card [071-0454]

[89] JCPD Card [042-0876]

[90, 91] R. T. Rajendra Kumar, B. Karunagaran, D. Mangalaraj, Sa. K. Narayandass, P. Manoravi, M. Joseph, Vishnu Gopal, R. K. Madaria, and J. P. Singh «DETERMINATION OF THERMAL PARAMETERS OF VANADIUM OXIDE UNCOOLED MICROBOLOMETER INFRARED DETECTOR», International Journal of Infrared and Millimeter Waves, Vol. 24, No 3, March 2003.

[92] Contribution de la diffraction de rayons X sous incidence rasante à l'étude de céramiques lustrées, January 2003, DOI: 10.3406/arsci.2003.1047.

[93] Yao Jina, Hitesh A. Basantania , AdemOzcelika, Tom N. Jacksonb, and Mark W. Horna «High Resistivity and High TCR Vanadium Oxide Thin Films For Infrared

Imaging Prepared by Bias Target Ion Beam Deposition» Proc. of SPIE Vol. 8704 (2013), doi: 10.1117/12.201627.

[94] Henry H. Radamson and M. Kolahdouz “Group IV Materials for Low Cost and High Performance Bolometers”, https://www.researchgate.net/publication/280777702.